Journal of the Mississippi Academy of Sciences

Volume 60 July 2015 Number 3

The Journal of the Mississippi Academy of Sciences (ISSN 0076-9436) is published in January (annual meeting abstracts), April, July, and October, by the Mississippi Academy of Sciences. Members of the Academy receive the journal as part of their regular (nonstudent) membership. Inquiries regarding subscriptions, availability of back issues, and address changes should be addressed to The Mississippi Academy of Sciences, Post Office Box 55709, Jackson, MS 39296-5709, telephone 601-977-0627, or email msacademyofscience@comcast.net.

Comment

Research Articles

Departments

COMMENT

BIOMEDICAL RESEARCHERS SHOULD DECLARE THEIR ASSUMPTIONS

Jerome Goddard[1] and Jerome Goddard II[2]

[1]Department of Biochemistry, Molecular Biology, Entomology, and Plant Pathology, Mississippi State University, Mississippi State, MS 39762
[2]Department of Mathematics and Science, Auburn University Montgomery, Montgomery, AL 36117

E-mail: jgoddard@entomology.msstate.edu

Recently, the Editor-in-Chief of *Science* asked its reviewers and editors to identify papers submitted to the journal that demonstrate excellence in transparency and instill confidence in the results (McNutt 2014). This was done in response to issues with irreproducibility (primarily) in preclinical studies. There may be other ways scientific papers can be made more transparent and reliable. Sometimes very solid, or at least well-intentioned, scientific reports contain assumptions which, if false, severely weaken the work. Assumptions are facts taken for granted, and in an argument, assumptions must be allowed as true for that particular argument to advance. Calling assumptions into question is a legitimate way to undermine a claim or simply deepen our understanding of the issue; however, if assumptions are never identified (declared), then spurious claims sometimes may be advanced as fact. One example of this occurred in a 1978 paper in *Nature* that is frequently quoted concerning cultural evidence of dog domestication. That letter reported a human skeleton found in a grave in what is now Israel with its hand resting on the chest of a puppy skeleton (Davis and Valla 1978) and the authors interpreted this as evidence of affection between the human and the dog. They said, "The puppy, unique among Natufian burials, offers proof that an affectionate rather than gastronomic relationship existed between it and the buried person." Offers *proof*? Several assumptions are actually necessary to draw this conclusion which were not identified in the paper: 1) that the puppy was purposely buried with the human, 2) that the hand was intentionally placed on the puppy, and 3) that this placement meant affection or familiarity between the two. Any one of these assumptions could have been false. In our opinion, readers of scientific and/or biomedical papers would benefit from a brief textbox or section at the beginning of each paper wherein underlying assumptions are disclosed. Mathematicians know all too well the dangers of hidden assumptions. There is perhaps no other discipline that can so readily prerequisite the importance of clearly stating *all* relevant assumptions. The counterpart in mathematics of hypothesis-driven experimentation and conclusion is the statement of proposition (or theorem) with a corresponding proof using formal logic. In this paradigm, the current setting (or global assumptions) and assumptions related to the problem at hand are carefully crafted and explicitly listed. From these assumptions and previously established results, the desired result may be deduced through an application of formal logic (proof by induction is an exception). Making a false assumption, either explicitly or implicitly, will always lead to erroneous results. Thus, it is a common practice in mathematics papers to *a priori* list all of assumptions regarding the proposition to be stated and proved (Lee 2010). Perhaps biologists should do the same.

REFERENCES

Davis, S. J. M., and F. R. Valla. 1978. Evidence for domestication of the dog 12,000 years ago in the Natufian of Israel. Nature 276: 608-610.

Lee, K. P. 2010. A guide to writing mathematics. http://www.cs.ucdavis.edu/~amenta/w10/writingman.pdf

McNutt, M. 2014. Reproducibility. Science (Editorial) 343: 229.

PLASMONIC NANOCRYSTALS WITH PRECISE GOLD ATOMS

Chanaka Kumara,[1] Xiaobing Zuo,[2] David A. Cullen,[3] Amala Dass[1,*]

[1]Department of Chemistry and Biochemistry, University of Mississippi, Oxford, Mississippi 38677, United States

[2]X-ray Science Division, Advanced Photon Source, Argonne National Laboratory, Argonne, Illinois 60439, United States

[3]Materials Science and Technology Division, Oak Ridge National Laboratory, Oak Ridge, Tennessee 37831, United States

ABSTRACT

Plasmonic nanoparticles have potential application in nano-optics, solar cell, catalysis, drug delivery and cancer treatment. Among those, thiol protected gold nanocrystals draw greater attraction due to their superior stability and ability to control the composition with atomic precision. However, the challenges in the synthetic protocol and lack of atom quantification techniques hinder the determination of atomic composition. For the first time, we were able to determine the atomic composition of the three different gold nanoparticles in the size regime of 2-4 nm. The composition was found to be $Au_{329}(SR)_{84}$, $Au_{\sim500}(SR)_{\sim120}$ and $Au_{\sim940}(SR)_{\sim160}$ by electro-spray ionization mass spectrometry. All of these nanocrystals exhibit surface plasmonic resonance at around ~500 nm. Size-dispersity of the gold nanocrystals was confirmed by mass spectrometry, synchrotron based small angle X-ray scattering and scanning transmission electron microscopy analysis. Possible atomic arrangements of these nanocrystals were determined by high-energy X-ray based pair distribution function analysis. These largest gold nanocrystals with known composition will pave the way to the understanding the origin of surface plasmon resonance and will have greater potential towards application in catalysis and optical devices.

INTRODUCTION

Surface plasmon resonance (SPR) is a collective oscillation of the free electron density of the metal with the incident radiation (1). Gold nanoparticles shows SPR at 500-550 nm depend on their shapes and size. Synthesis and characterization of small colloidal gold nanoparticles, where molecule-to-plasmonic transitions occur, is hindered by polydispersity and spontaneous particle aggregation (2). However, thiol protected gold nanocrystals draw greater attraction due to their ultra-stability and ability to control their composition with atomic precision (3).There are two size regimes within thiol-protected gold nanoparticles (a) ultra-small gold nanomolecules, which are less than 2 nm in diameter and (b) plasmonic nanocrystals, which are larger than 2 nm and exhibit surface plasmon resonance.

Atomically precise ultra-stable gold nanoparticles such as $Au_{25}(SR)_{18}$ (4), $Au_{38}(SR)_{24}$ (5), $Au_{130}(SR)_{50}$ (6), $Au_{137}(SR)_{54}$(7), and $Au_{144}(SR)_{60}$ (8) (where the R group is thiol ligand attached) have previously been prepared with atomic precision using the Brust-Schriffin method. However, these synthetic protocols were only applicable to ultra small gold nanoparticles and limited control was achieced for larger nanoparticles (9,10).

The most promising techniques used in compositional analysis of these nanoparticles are X-ray crystallography and mass spectrometry (MS) (11-14). However, structural analysis of plasmonic nanoparticles still remains challenging; polydispersity and larger particle size often prevent the diffraction quality single crystals. Nevertheless, advances in instrumental methods have developed in mass spectrometry (MS) techniques, such as MALDI and ESI for determination of the composition.

This report discuss the recent progress in super-stable plasmonic nanoparticles at 76.3, 115, 200 kDa mass range. Ultimately, Electro-spray ionization mass spectrometry window (ESI-MS) was able to expand upto 200 kDa mass range to determine the atomic composition of gold nanoparticles. These nanoparticles were characterized by suite of analytical techniques like synchrotron based small angle X-ray scattering (SAXS) and high-energy X-ray based pair distribution function analysis (PDF). Further, the monodispersity of the synthesized nanoparticles was verified using scanning transmission electron microscopy (STEM) analysis.

EXPERIMENTS

Synthesis: Atomically precise nanoparticles synthesis involves three steps. Initially, a crude mixture containing

polydisperse Au nanoparticles was prepared in a modified version of the previous report (15). Then, meta-stable nanoparticles were eliminated by thermochemical treatment of the crude product with excess thiol (16). Finally, pure monodisperse nanopartilces were isolated by solvent fractionation.

Step1: Aqueous solution (30 mL) of $HAuCl_4$ (0.1772 g/0.45 mmol) and toluene solution (30 mL) of tetraoctylammonium bromide, TOABr (0.55 mmol) were mixed and stirred well (30 min). Phenylethanethiol (0.0622 mL/0.225 mmol) was added to the separated organic phase, and further stirred at room temperature (for 30 min). Gold to thiol molar ratio was varying 1:1, 1:0.5 and 1:0.25 depending on the desired final product. An aqueous solution of $NaBH_4$ (10 mmol, 20 mL) cooled to 0 °C, was added to the reaction mixture and stirred for another 2 h. Then, organic layer was separated and evaporated to dryness. The product was washed with methanol three times to remove thiol and other byproducts.

Step 2: Around ~100-200 mg of the crude product was dissolved in toluene 90.50 mL) and subjected to thermochemical treatment with excess phenylethanethiol (0.05 mL) at 80° C under stirring while monitoring the product with MALDI-MS. After several days of etching, product was washed with methanol several times, and extracted with toluene.

***Step 3*:** Then nanoparticles were dissolved in toluene and subjected to solvent fractionation to isolate the desired nanoparticles at 76.3,115 and 200 kDa (Figue 1).

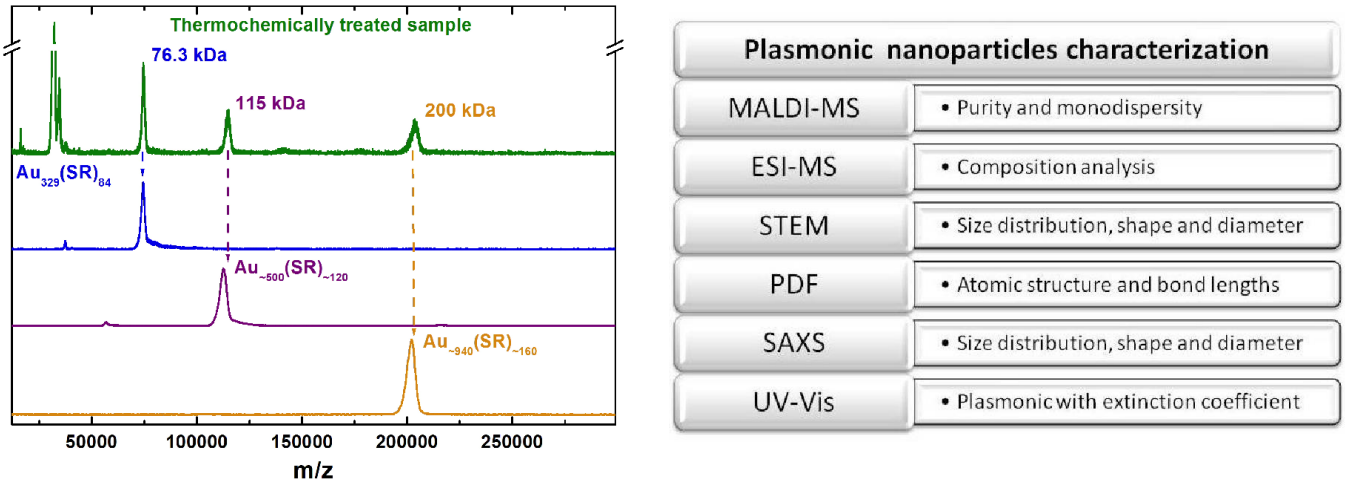

Figure 1: (left) MALDI-MS of the thermochemically treated product and isolated nanoparticles at 76,115 and 200 kDa. Adapted from ref [17] (right) Suite of technique used for characterization of plasmonic gold nanoparticles. MALDI-MS: Matrix assisted laser desorption ionization mass spectrometry, ESI-MS: Electro-spray ionization mass spectrometry, STEM: Scanning transmission electron microscopy, PDF: pair distribution function analysis, SAXS: Small angle X-ray scattering, UV-vis: Ultraviolet-visible absorption spectroscopy.

RESULTS AND DISCUSSION

Wet-chemical methods were developed and optimized for synthesis of atomically monodisperse plasmonic gold nanoparticles. These nanoparticles subjected to the complete and comprehensive characterization using mass spectrometry, spectroscopy, high resolution electron microscopy and X-ray diffraction tools. Following content will composition assignment and characterization of 76.3,115 and 200 kDa.

Plasmonic Au329(SR)84 nanoparticles

The main objective of this work is to determine the chemical composition of the previously reported large 76.3 kDa thiolated gold nanomolecules (15). This is the smallest sized nanoparticles that exhibit surface plasmonic resonance. First, the purity of the sample was determined by MALDI-TOF mass spectrometry. Figure 2a, STEM of identical size particles and Figure 2b.c, MALDI spectra shows clear baseline indicating nascence absence of any other nanoparticles or detectable impurities. It is well established that the nanoparticles with fixed atomic composition can be synthesized utilizing the different ligand that have similar properties but different in mass. For example composition of $Au_{38}(SR)_{24}$, $Au_{67}(SR)_{35}$ and $Au_{144}(SR)_{60}$ are independent of different -R groups. In other words, if one can make the same nanoparticles with different ligand, mass difference method can be applied to determine the composition of newly synthesized nanoparticles. Figure

2d shows the expansion of the 3- region of the ESI mass spectrometry of the 76.3 nanoparticles synthesized using three different thiols namely −SC6H13(117 Da), −SCH2CH2Ph (137 Da), and−SC12H25(201 Da). In each case, gold to thiol compositional assignment yielded 329:84.18 Both positive and negative mode of ESI-MS spectra show identical peaks indicating the absence of any other counter ions (Figure 2e). Cesium acetate is commonly added to the nanoparticles to promote the ionization in mass spectrometric analyses by forming Cs adduct. Therefore, Cs+ ions were intentionally added to prove that the $Au_{329}(SR)_{84}$ is the base molecular ion. In this case envelope of peaks due to several cesium adducts (1 to7 Cs ions) were observed.

A comprehensive investigation including the analysis of nanoparticles with three ligands, in positive and negative mode and Cs+ adduction lead to a conclusive composition of $Au_{329}(SR)_{84}$. Based on the assigned formula, there are 245 free electrons to facilitate the surface plasmon resonance (the next smallest cluster $Au_{187}(SR)_{68}$ (6) which have 119 free electron does not support for SPR). Therefore, this compositional determination will facilitate the fundamental understanding of the birth of surface plasmon resonance (18).

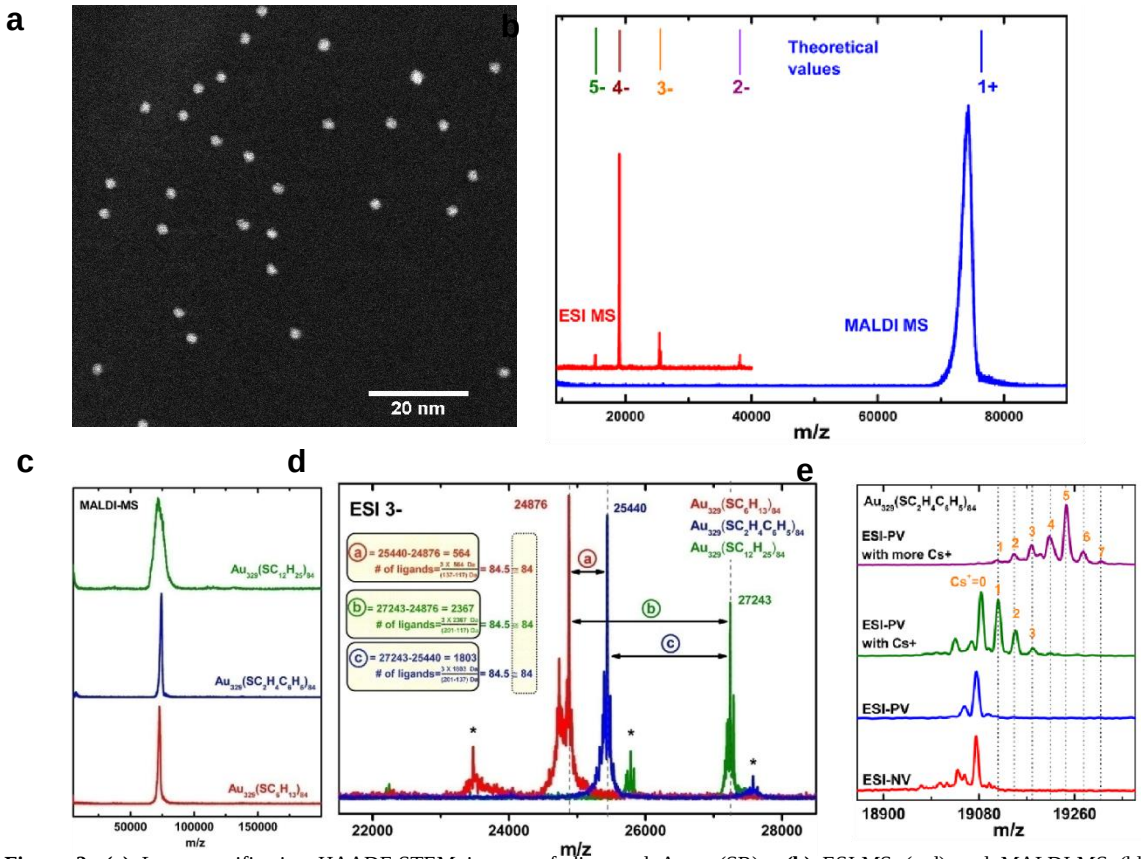

Figure 2: (a) Low-magnification HAADF-STEM images of dispersed $Au_{329}(SR)_{84}$**.(b)** ESI-MS (red) and MALDI-MS (blue) spectra of 76.3 kDa nanomolecules synthesized using $HSCH_2CH_2C_6H_5$ thiol. The lines at the top indicate the theoretical values for the 1, 2, 3, 4, and 5 charge states of $Au_{329}(SCH_2CH_2Ph)_{84}$. **(c)** Ligand count determination by analyzing 76.3 kDa species protected by various ligands. **(c)** MALDI-MS of the 76.3 kDa nanomolecules synthesized using dodecanethiol (olive), phenylethanethiol (blue), and hexanethiol (red). **(d)** ESI-MS Q-TOF of 3- ions of the 76.3 kDananomolecules using three ligands. Assuming that the number of metal atoms is constant, for the 76.3 kDa nanomolecule for these three ligands, the number of ligands is calculated by the mass difference of the intact ESI ions. The ligand count was found to be 84 in all cases, which then leads to the Au atom count of 329 atoms. Peaks marked by an asterisk indicate remaining impurities not removed during purification or other minor species present in the sample. Dotted lines indicate the theoretical mass of the 3−ions of corresponding $Au_{329}(SR)_{84}$ nanomolecules. **(e)** $Au_{329}(SCH_2CH_2C_6H_5)_{84}$ with negative mode (NV, red) and positive mode (PV, blue) in the presence of cesium acetate (PV, olive) and further addition of cesium acetate (PV, purple). The positive and negative spectra shows the 4+ and 4−molecular ions, respectively, while the addition of cesium acetate leads additional peaks due to the formation of Cs^+ adducts, such as $Au_{329}(SCH_2CH_2C_6H_5)_{84}\cdot Cs^+$,$Au_{329}(SCH_2CH_2C_6H_5)_{84}\cdot 2Cs^+$, $Au_{329}(SCH_2CH_2C_6H_5)_{84}\cdot 3Cs^+$. Further addition of cesium acetate leads to adducts with 4, 5, 6, and 7 Cs^+ ions. Reprinted with permission from [18]. Copyright 2014 American Chemical Society.

Plasmonic Au~500(SR)~120 nanoparticles

Experimental conditions were optimized for synthesis and isolation of next largest super stable plasmonic gold nanoparticles at 115 kDa. In this case Au:thiol ratio set to 1:0.5, instead of 1:1. We were able to synthesize these nanoparticles with two different ligands (phenylethanethiol and hexanethiol). Ligand mass difference method was employed to determine the atomic composition using ESI mass spectrometry. First the number of ligands was determined as 120, using ligand mass difference method and then number of gold atoms were back calculated and found to be 500.

However, broader mass peaks were observed when compared to the ultra-small nanoparticles. This is due to the several stable species within 115 kDa mass range. Control experiments were performed with Au329 which shows fixed composition, to verify the size dispersity of the 115 kDa mass range. Based on the ESI-MS peak width, composition was concluded to be Au~500±10(SCH2CH2Ph)~120±3.

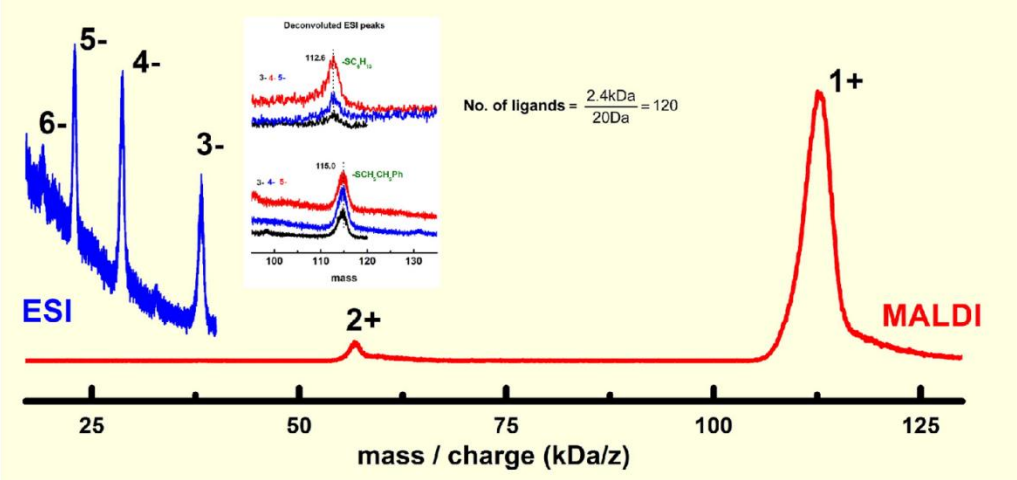

Figure 3: Mass Spectrometry. MALDI (red) and ESI (blue) mass spectra of "115 kDa" nanoparticles yielding a composition of Au~500±10(SCH2CH2Ph)~120±3. MALDI-MS shows 1+ and 2+ ions, while ESI yields 3−,4−,5−, and 6−ions. Deconvolution of the six charged ions is consistent with a 115 kDa molecular ion. The inset shows the deconvoluted spectra of Au~500 protected by−SCH2CH2Ph and−SC6H13 ligands, where the 3−,4−, and 5−ESI peaks are multiplied by 3, 4, and 5 to yield the 1−molecular ion, at 115 kDa. From the mass difference, the total number of ligands was calculated to be 120. Reprinted with permission from [19]. Copyright 2014 American Chemical Society.

HAADF-STEM (Figure 4) shows the monodisperse, hexagonal shaped 2.4± 0.1 nm particles with FCC planes. Sintering and electron beam induced nanoparticles aggregation directly effect to the observed nanoparticles size, shape and size dispersity. Surface atom diffusion and reconstruction were observed with HAADF-STEM imaging as a result of high electron dose. Thus beam dose was optimized and minimized using lower voltage and acquiring first-pass images. Figure 4 a, b and c show the representative low-magnification images of the particles. The images visually demonstrate the monodispersity and self-assembled particles on the TEM grid. Figure 4d−h show the high resolution images of the isolated $Au_{\sim 500}(SR)_{\sim 120}$ nanoparticles, illustrating the surface morphology of individual $Au_{\sim 500}$ nanoparticles.

High energy X-ray based atomic pair distribution function shows the histogram of the entire atom–atom distances within the single nanoparticles. Total scattering measurements account for both Bragg and diffuse scattering and its fourier transformation into real space yields the PDF. Figure 5(left) shows the synchrotron high energy X-ray-based pair distribution function analysis of $Au_{\sim 500\pm 10}(SR)_{120\pm 3}$ in comparison with fcc-like 100 nm gold nanoparticles, calculated PDF of icosahedral Au_{309} ,Marksdecahedral Au_{389}, and truncated octahedral Au_{405}. Experimental PDF data matches with the Marksdecahedral, and truncated octahedral models. Figure 5(right) shows the SAXS data and analysis will provide the shape, size and size dispersity information of the $Au_{\sim 500}(SR)_{\sim 120\ system}$. The wide range of linear Guinier behavior (ln[I(q)] vs 2, Figure 5b inset) at low scattering angles and the scattering features from 0.3−0.8 Å−1 depict the monodispersity of the Au~500 nanoparticles. Three-dimensional molecular envelopes were reconstructed from the SAXS data and envelope adopts an ellipsoid-like shape (dimensions of 2.2−3.0 nm). The diameter measured by small angle X-ray scattering was

2.6 ± 0.2 nm, which is in agreement with TEM and PDF measurements.

Plasmonic peaks for these particles appear at ~498 nm. SPR is supported by 380 free electrons based on composition assignment. These plasmonic nanoparticles can be used in plasmonic application such as optical sensors, drug delivery, cancer cell detection and also in catalytic applications.

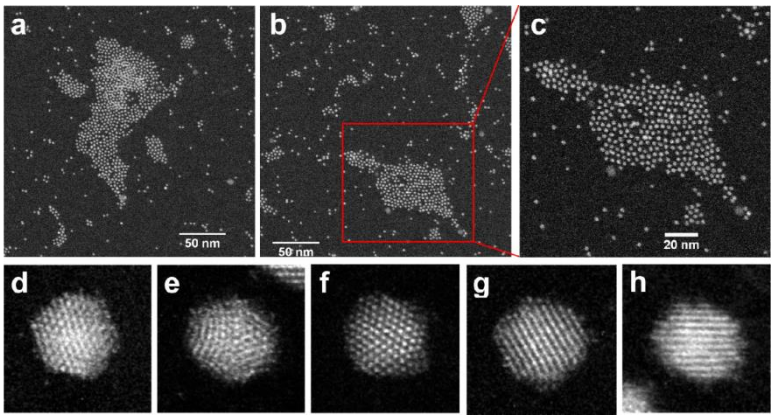

Figure 4. HAADF-STEM images of Au~500(SR)~120. (a–c) Low-magnification images of dispersed Au~500(SR)~120. (d–h) High-resolution images of individual particles, field of view is 5 nm × 5 nm. Reprinted with permission from [19]. Copyright 2014 American Chemical Society.

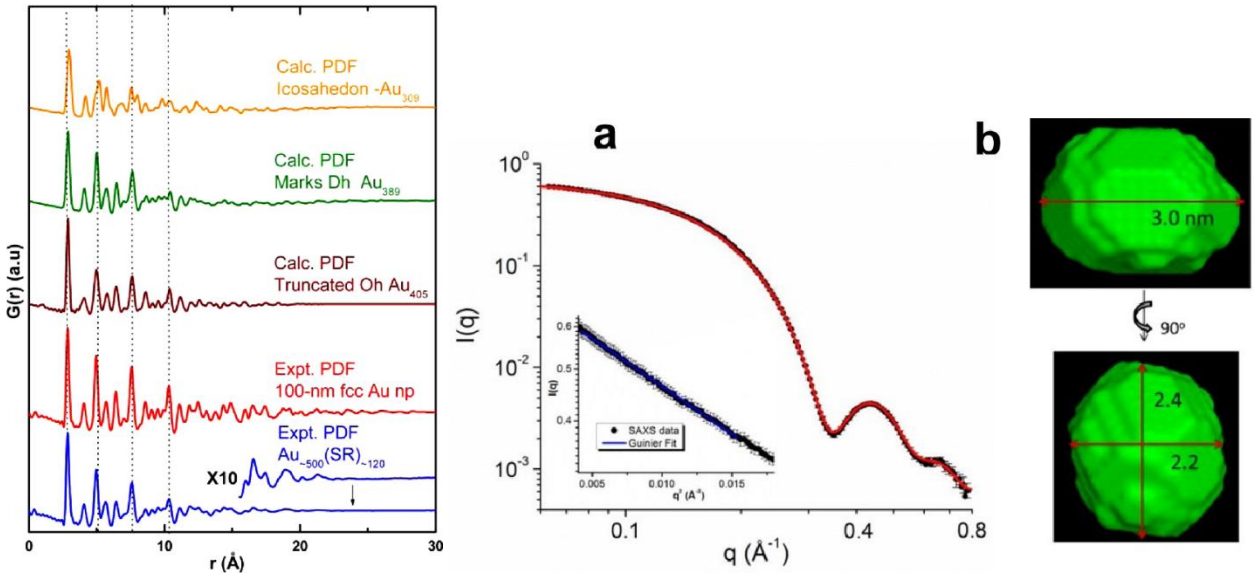

Figure 5:(Left) Experimental atomic PDF of Au~500±10(SR)120±3 in comparison with calculated PDF patterns of icosahedral Au309, Marks Dh Au389, Truncated Oh Au405 and 100 nm fcc (bulk like) patterns. PDF patterns of Au~500 show a decent match with Marks Dh and fcc patterns. **(Right)** SAXS data, data fits, and the derived SAXS molecular envelope for Au~500 nanoparticles. **(a)** SAXS data (black solid circle with error bar) were collected up to 0.8 Å−1. The red curve is a representative fit for the molecular envelope calculation. The molecular envelope, also known as a bead model, wascalculated using the program DAMMIN, with SAXS data up to 0.6 Å −1. The data points in the red curve beyond 0.6 Å−1 were calculated from the resultant molecular envelope, matching well with the experimental data. The inset is the Guinier fit for SAXS data at q close to 0. Rg obtained from the data fit is 1.05±0.05 nm. **(b)** The two views of the final SAXS molecular envelope with dimensions. Twenty independent molecular envelope calculations were performed, and the resulting envelopes were further averaged to generate the final, consensus molecular envelope. The error bar of the dimensions is expected as 0.1−0.2 nm. Reprinted with permission from [19]. Copyright 2014 American Chemical Society.

Plasmonic $Au_{\sim 940}(SR)_{\sim 160}$ nanoparticles

Experimental conditions were further modified to synthesize the next largest super stable plasmonic gold nanoparticles at 200 kDa. Au:thiol ratio further reduced to 1:0.25 to yield the gold nanoparticles at 200 kDa. Figure 6 shows the MALDI (blue) and ESI (red) mass spectra of the gold nanoparticles synthesized using phenylethanethiol. Mass peak at 200 kDa shows the monodispersity of the sample and the flat base line implies the absence of other impurities. Inset shows the deconvoluted ESI-MS of the nanoparticles with phenylethanethiol and hexanethiol ligands. Mass different method yielded, the assignment of Au~940SR~160. This is the largest size to be characterized by high resolution ESI mass spectrometry.

Low-magnification STEM images of the $Au_{\sim 940}(SR)_{\sim 160}$ particles show the monodispersity of the particles. Furthermore, the atomic structure was studied in high-resolution STEM images. HAADF-STEM images show fcc-like, 2.9 nm particles. Figure 7.j shows the Fast Fourier transform (FFT) of the single nanoparticles in 3i. The measured FFT lattice spacing are closely match with the bulk fcc.

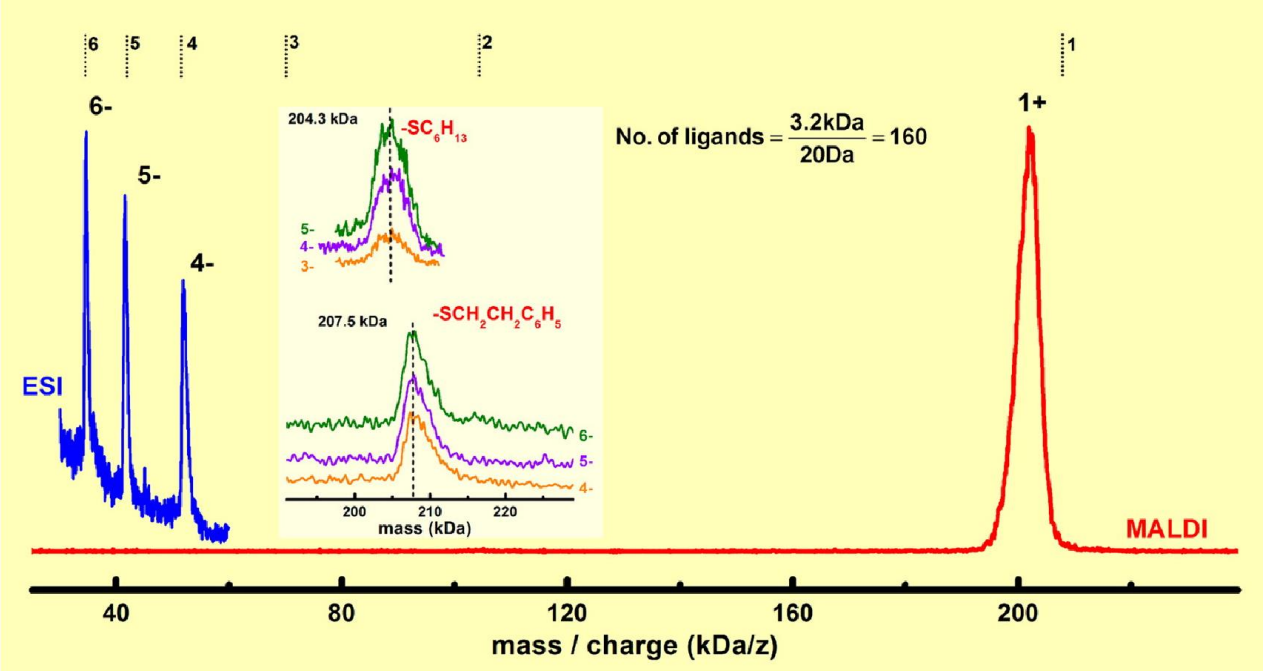

Figure 6: Mass spectrometry. MALDI (red) and ESI (blue) mass spectra of 207 kDa nanoparticles synthesized using HSCH2CH2Ph thiol. MALDI-MS with DCTB matrix shows 1+ ions, while ESI-MS yields 4–, 5–, and 6– multiply charged ions. The theoretical values for charge states 1, 2, 3, 4, 5, and 6 are shown by dotted lines at the top. The inset shows the deconvoluted ESI mass spectra of 940 atom nanoparticles protected by −SC6H13 and −SCH2CH2Ph. The deconvolution of the multiply charged ions (4–, 5–, and 6– ESI peaks are multiplied by 4, 5, and 6, respectively, to yield the 1– molecular ion at 207.5 kDa for the –SCH2CH2Ph ligand) of the multiply charged ions. This mass difference was used to calculate the number of ligands. The composition of the nanoparticles was determined to be Au940±20(SR)160±4. Reprinted with permission from [17]. Copyright 2014 American Chemical Society.

Figure 8(left) shows the high energy X-ray based atomic pair distribution function (PDF) data of the $Au_{\sim 940}(SR)_{\sim 160}$ in comparison with fcc-like 100 nm gold nanoparticles, calculated PDF of icosahedral Au_{923}, marksdecahedral Au_{831} and truncated octahedral Au_{807} models. Experimental PDF data significantly matches with the calculated truncated octahedral Au807 model. The Au_{807} model consists of 13, 42, 92, 162, 252, and 246 atoms in each individual shell (Figure 8a). The 3-D molecular envelope were derived from the $Au_{\sim 940}(SR)_{\sim 160}$ SAXS data shows an 3.3 nm sized ellipsoid-like shape and the cross section of about 2.5-2.8 nm. The diameter measured by SAXS, 3.0 ± 0.2 nm, is in agreement with STEM particle diameter measurements (Table 1). UV-visible spectrum shows the SPR at 506 nm which is supported by around 780 free electrons based on composition assignments.

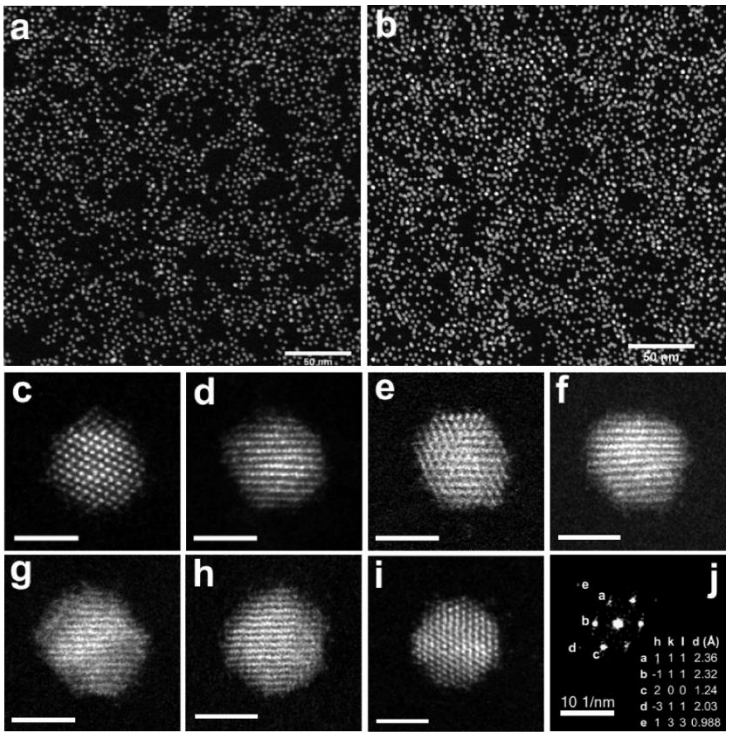

Figure 7: Electron microscopy. STEM images of the Au~940(SR)~160 nanoparticles. (a,b) Low-magnification STEM images. (c–i) High-resolution HAADF-STEM image of the individual nanoparticles, scale bar is 2 nm. (j) Fast Fourier transform of (i) showing lattice spots similar to bulk fcc Au oriented along the [0–11] zone axis. Reprinted with permission from [17]. Copyright 2014 American Chemical Society.

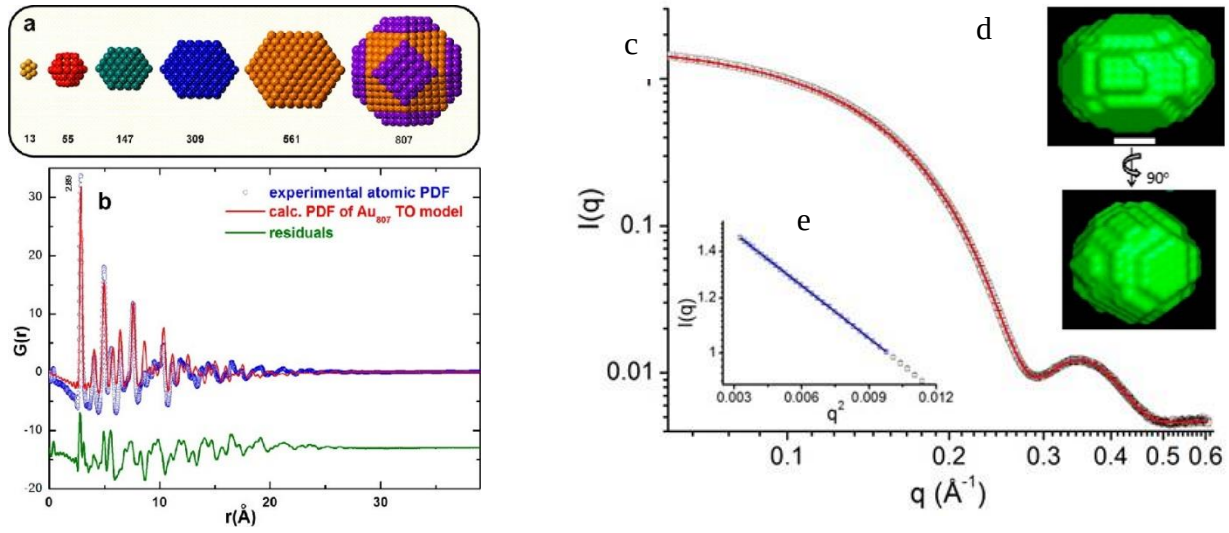

Figure 8: (Left) (a) Proposed six-shell Au_{807} atomic model for the metal-core-only portion of $Au_{\sim 940}(SR)_{\sim 160}$ nanoparticles. **(b)** PDF fit of the Au807 TO model with that of the experimental PDF of Au~940(SR)~160. The *R*w is 44%. Note that the model only considers the metal core. **(Right)** SAXS data, fittings, and the derived SAXS molecular envelope of Au_{940} nanoparticle. **(c)** SAXS data (black open circle with error bar) were collected up to 0.6 Å-1. The red curve is a representative fitting in the molecular envelope calculation. The molecular envelope, also known as bead model, was calculated using the program DAMMIN, with SAXS data up to 0.6 Å-1. **(d)** The inset is the Guinier fit for SAXS data atqclose to 0.Rg obtained from the fitting is 1.32±0.07 nm. **(e)** Two views of the final SAXS molecular envelope. The length of the white bar is 1.0 nm. Reprinted with permission from [17].

CONCLUSIONS

The composition of the plasmonic gold nanoparticles at 76.3, 115 and 200 kDa were assigned to be $Au_{329}(SR)_{84}$, $Au_{\sim 500}(SR)_{\sim 120}$, $Au_{\sim 940}(SR)_{\sim 160}$ based on high-resolution mass spectrometric studies. Composition determination here will facilitate the theoretical and experimental studies on origin of SPR and atomic model to understand the properties of nanoparticles. Nanoparticles size, atomic structure and optical absorbance information has summarized in the following table

Table 1: Properties of plasmonic nanoparticles as determined by the comprehensive analytical tools.

Composition§	SAXS dia.(nm)	TEM dia. (nm)	Atomic structure†	Optical absorbance (nm)
$Au_{329}(SR)_{84}$	2.2 ± 0.2	2.0 ± 0.1	close packed	490
$Au_{500\pm10}(SR)_{120\pm3}$	2.6 ± 0.2	2.4 ± 0.1	close packed	498
$Au_{\sim 940\pm20}(SR)_{\sim 160\pm4}$	3.0 ± 0.2	2.9 ± 0.1	close packed	506

§from mass spectrometry

ACKNOWLEDGEMENTS

C.K. gratefully acknowledges Prof. Amala Dass for his advising, guiding and supporting over the years. C.K. thank to the financial support from NSF CHE-1255519. C.K. also thanks Karena Chapman for PDF data collecting, Xiaobing Zuo for SAXS and David Cullen for STEM data collection and analysis. Work performed at Argonne and the use of the Advanced Photon Source, an Office of Science User Facility operated for the U.S. Department of Energy (DOE) Office of Science by Argonne National Laboratory, was supported by the U.S. DOE under Contract No. DE-AC02- 06CH11357. Electron microscopy research was supported through a user project supported by ORNL's Center for Nanophase Materials Sciences (CNMS), which is sponsored by the Scientific User Facilities Division, Office of Basic Energy Sciences, U.S. Department of Energy.

LITERATURE CITED

1. Hu M, et al. Gold nanostructures: engineering their plasmonic properties for biomedical applications. Chemical Society Reviews 35, 1084-1094 (2006).
2. Parker JF, Fields-Zinna CA, Murray RW. The Story of a Monodisperse Gold Nanoparticle: Au25L18. Accounts of Chemical Research 43, 1289-1296 (2010).
3. Walter M, et al. A unified view of ligand-protected gold clusters as superatom complexes. Proceedings of the National Academy of Sciences 105, 9157-9162 (2008).
4. Heaven MW, Dass A, White PS, Holt KM, Murray RW. Crystal Structure of the Gold Nanoparticle [N(C8H17)4][Au25(SCH2CH2Ph)18]. Journal of the American Chemical Society 130, 3754-3755 (2008).
5. Qian H, Eckenhoff WT, Zhu Y, Pintauer T, Jin R. Total Structure Determination of Thiolate-Protected Au38 Nanoparticles. Journal of the American Chemical Society 132, 8280-8281 (2010).
6. Negishi Y, Sakamoto C, Ohyama T, Tsukuda T. Synthesis and the Origin of the Stability of Thiolate-Protected Au130 and Au187 Clusters. The Journal of Physical Chemistry Letters 3, 1624-1628 (2012).
7. Jupally VR, et al. Au137(SR)56 nanomolecules: composition, optical spectroscopy, electrochemistry and electrocatalytic reduction of CO2. Chemical Communications 50, 9895-9898 (2014).
8. Lopez-Acevedo O, Akola J, Whetten RL, Grönbeck H, Häkkinen H. Structure and Bonding in the Ubiquitous Icosahedral Metallic Gold Cluster Au144(SR)60. The Journal of Physical Chemistry C 113, 5035-5038 (2009).
9. Whetten RL, et al. Nanocrystal gold molecules. Advanced Materials 8, 428-433 (1996).
10. Hostetler MJ, et al. Alkanethiolate Gold Cluster Molecules with Core Diameters from 1.5 to 5.2 nm: Core and Monolayer Properties as a Function of Core Size. Langmuir 14, 17-30 (1998).
11. Ferrando R, Jellinek J, Johnston RL. Nanoalloys: From Theory to Applications of Alloy Clusters and Nanoparticles. Chemical Reviews 108, 845-910 (2008).
12. Dass A, Dubay GR, Fields-Zinna CA, Murray RW. FAB Mass Spectrometry of Au25(SR)18 Nanoparticles. Analytical Chemistry 80, 6845-6849 (2008).
13. Dass A, Stevenson A, Dubay GR, Tracy JB, Murray RW. Nanoparticle MALDI-TOF Mass Spectrometry without Fragmentation: Au25(SCH2CH2Ph)18 and Mixed Monolayer Au25(SCH2CH2Ph)18−x(L)x. Journal of the American Chemical Society 130, 5940-5946 (2008).

14.Jadzinsky PD, Calero G, Ackerson CJ, Bushnell DA, Kornberg RD. Structure of a Thiol Monolayer-Protected Gold Nanoparticle at 1.1 Å Resolution. Science 318, 430-433 (2007).

15. Dass A. Faradaurate Nanomolecules: A Superstable Plasmonic 76.3 kDa Cluster. Journal of the American Chemical Society 133, 19259-19261 (2011).

16. Schaaff TG, Whetten RL. Controlled Etching of Au:SR Cluster Compounds. The Journal of Physical Chemistry B 103, 9394-9396 (1999).

17. Kumara C, Zuo X, Cullen DA, Dass A. Faradaurate-940: Synthesis, Mass Spectrometry, Electron Microscopy, High- Energy X-ray Diffraction, and X-ray Scattering Study of Au~940±20(SR)~160±4 Nanocrystals. ACS Nano 8, 6431-6439 (2014).

18. Kumara C, Dass A. Au329(SR)84 Nanomolecules: Compositional Assignment of the 76.3 kDa Plasmonic Faradaurates. Analytical Chemistry 86, 4227-4232 (2014).

19. Kumara C, Zuo X, Ilavsky J, Chapman KW, Cullen DA, Dass A. Super-Stable, Highly Monodisperse Plasmonic Faradaurate-500 Nanocrystals with 500 Gold Atoms: Au~500(SR)~120. Journal of the American Chemical Society 136, 7410-7417 (2014).

LEARNING ABOUT ENZYME SPECIFICITY WITH AN INTERACTIVE ENZYME MODEL: INFLUENCES ON STUDENT MOTIVATION, COGNITIVE LOAD, AND ACHIEVEMENT

Mounir R. Saleh, Sherry S. Herron, Kyna Shelley, and Robert Bateman

University of Southern Mississippi, Hattiesburg, MS and William Carrey Univeristy, Hattiesburg, MS

ABSTRACT

Scientists' progress in understanding enzyme specificity uncovered a complex natural phenomenon. However, not all of the currently available biology textbooks seem to be up to this progress. Nevertheless, students' understanding of how enzymes work is related to understanding other biological processes like receptor-ligand interactions. In an attempt to bridge this gap, we developed some instructional material consisting of a worksheet and an interactive physical model. The worksheet is structured based on the "segmentation principle" which is meant to meet the complexity of scientific processes like the one in hand (Mayer, 2009). The model in turn is primarily designed to visualize the process as well as promote motivation to learn about it. We describe here a case study in which we used this instructional material and examined its contribution to promote motivation and understanding of enzyme specificity on 30 undergraduate students majoring in life sciences-related fields.

INTRODUCTION

One of the main aspects of the nature of science is tentativeness of scientific information. A good example from biochemistry is the replacement of the old "lock and key" model of enzyme specificity (Fischer, 1894) by the "induced fit" model (Koshland, 1958). However, a quick search on the concept of enzyme specificity in some of the widely used high school biology textbooks revealed inconsistent representations of our current understanding of how enzymes work. As can be seen in (Figure.1), 83.3% of examined textbooks (total of twelve) failed to simultaneously discuss the basic elements of the concept, (1) conformational change and (2) chemical interaction between the substrate and catalytic amino acids. Particularly, only 60% covered the role of conformational change in text while 50% visually represented it. Also, a mere of 20% touched on the chemical basis of the phenomenon while 10% represented the interaction in figures. This is not to mention the complete absence of other concept elements like binding affinity and enzyme reactivity which may be argued to be only relevant to upper college levels.

Having known this, it is not surprising that only one of the eight senior college students that we interviewed prior to this study seemed to have heard about the "induced fit" model in previous biology courses (Saleh et al., 2013). Mind that this concept is directly related to understanding other important areas in science, such as how some pharmaceutical drugs work on certain life-threatening diseases and the role of some mutations in causing inherited metabolic disorders, let alone comprehending other biological mechanisms at the molecular level (e.g. ligand-receptor specificity).

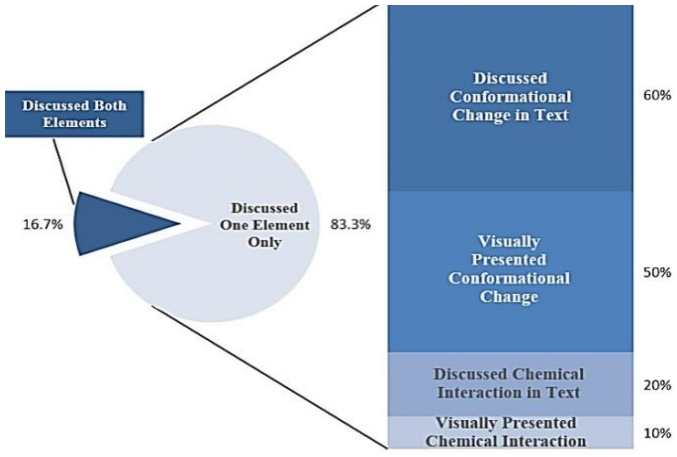

Figure.1: Bar of a Pie Chart Showing Inconsistency in Concept Representation

Nevertheless, addressing this problem is a twofold challenge. First, the old concept is easy to comprehend partly because it is represented through a very familiar example "lock and key." On the other hand, the new concept describes enzyme specificity as a complex process with various interacting parts that cannot be learned in isolation (Pollock et al, 2002). For example, to understand enzyme specificity, students need to simultaneously learn that binding of a substrate to its enzyme drives the latter to undergo a proper conformational change necessary to align the various catalytic amino acid residues in the active site along with the appropriate reactive groups of this substrate. In other words, they need to simultaneously consider the various elements and their possible interactions. As a consequence, such complex material may impose high cognitive load on the learner's working memory who may end up de-motivated to learn about it (Sweller & Chandler, 1994; Marcus, Cooper, & Sweller, 1996).

Second, for the "lock and key" model, a visual aid -*if any*- has to be static *at most* for students to grasp the idea of "how enzymes work." However, the current model defines enzymes as dynamic entities in whole and in parts. This entails another source of cognitive load necessary to mentally visualize the appropriate model; a requirement that might also overload the learner's working memory (Schonborn & Anderson, 2006).

For the purpose of meeting the first challenge, we studied literature that deals with learning complex material and chose applying the "segmentation principle" to our case (Mayer, 2009). This principle states that people learn complex processes better in learner-paced segments rather than in a single continuous unit.

To further help students understand the concept with minimum cognitive load (Vekiri, 2002), and be motivated to learn about it (Mayer, 2009), the first author built an interactive physical model representing the enzyme along with different pieces corresponding to different substrates; all of which go along with the worksheet as a single instructional material (US Patent Application No. 29508018). We intentionally avoided adding interesting but irrelevant features (e.g. smiley eyes) to the enzyme model assuming that they may be detrimental to the learning process (Lehman et al., 2007), let alone that otherwise the model would have been perceived as too juvenile by college students (Figure.2).

We would like to note that, in this article, we do not intend to analyze the theoretical basis of the "segmentation principle" or study how visual tools help enhance learning submicroscopic processes, like enzymes under action.

Figure.2: Enzyme Model

Rather, we aim to share an interactive lesson we found effective, cognitively efficient, and motivating for college students coming from various life sciences-related fields. We first discuss instruments used to measure students' reported mental effort, motivation, and achievement. We then describe our intervention and discuss its outcomes based on these three measures. Additionally, we calculate Instructional Efficiency IE of this intervention in order to evaluate the cost of students' performance in terms of their reported mental effort *(*Kalyuga & Sweller, 2005; Paas & van Merrie¨nboer, 1993*)*. IE has shown to be a more indicative measure of the quality of instruction than conventional measures of achievement *(van Gog et al., 2008).*

INSTRUMENTS

To measure essential cognitive load needed to understand the material, we asked students "*Please rate your level of mental effort on this part of the lesson"* at eight points throughout the worksheet on a scale of 9-points ranging from 1 (*extremely low mental effort*) to 9 (*extremely high mental effort*) (DeLeeuw & Mayer, 2008). We chose four points in the worksheet with lowest complexity, where students have only to report one/two observations in the experiment (just before rating their mental effort), and four other points with highest complexity, where they have to draw out a conclusion/deduction based on their observations from previous experiments. We then computed Cronbach's alpha to investigate internal consistency of mental effort rating at both lowest and highest complexity points. The mean score of the eight points represents the overall essential cognitive load (mental effort) experienced during the learning session.

To measure students' motivation level, we adapted the popular Instructional Materials Motivation Scale (IMMS) (Keller, 1987). IMMS addresses the following subscales of motivation: attention, relevance, confidence, and satisfaction with the instructional material. The validity of this scale has been established at the college-level setting by Huang et al. (2006). The adapted instrument consists of 23 questions divided into subsections of 8 items on attention, 6 on relevance, 5 on confidence, and 4 on satisfaction (Table-1). We asked students to rate each question based on the following Likert scale: 1=Strongly disagree, 2=Disagree, 3=Neither disagree nor agree, 4=Agree, and 5=Strongly agree. We then considered the mean score as well as scores of subscales to describe students' motivation to learn about enzyme specificity through using our instructional material.

Table.1

Instructional Material Motivation Survey IMMS

Attention

1. There was something interesting about the Enzyme Model that got my attention.
2. This Enzyme Model is eye-catching.
3. The Enzyme Model helped to hold my attention.
4. The design of the Enzyme Model looks *boring*.
5. This Enzyme Model stimulated my curiosity.
6. The Enzyme Model helped me learn some important things about enzyme specificity.
7. The variety of pieces that came with the Enzyme Model *distracted* me.
8. The worksheet associated with the Enzyme Model was appropriate to understand about enzyme specificity.

Relevance

1. It is *not* clear to me how the Enzyme Model is related to the concept of enzyme specificity.
2. Completing this session successfully was important to me.
3. The concept of enzyme specificity was relevant to my major because I need to know about how enzymes work.
4. I could *not* relate the content of the worksheet associated with the Enzyme Model to my own coursework.
5. The content of the worksheet which comes with the Enzyme Model was useful to me.
6. The content of the worksheet which comes with the Enzyme Model will be useful to me.

Confidence

1. The concept of enzyme specificity was easier to understand through the Enzyme Model than I thought it would be.
2. I felt *confused* about what I was supposed to learn from this learning session while using the Enzyme Model.
3. I was *not* able to pick out and remember the important points.
4. After attending this learning session, I was confident that I would be able to do well in the post- test.
5. As I went through the worksheet, I was confident that I could learn the content.

Satisfaction

1. Completing this learning session, with the Enzyme Model, gave me a satisfying feeling of accomplishment.
2. I really enjoyed the Enzyme Model being used in class.
3. It was *confusing* to work on the worksheet.
4. It felt good to successfully complete this learning session.

Finally, we assessed students' knowledge about the concept before and after intervention through administering identical pre- and post-tests. Each test consists of 5 multiple choice items. All of these items are "*Remember"* questions (Anderson et al., 2001) that we examined for face validity and internal reliability. Below is a sample test item:

Glucose is the original substrate for the enzyme Hexokinase. 3-methyl Glucose is an analogue to Glucose. See both substrates below:

Glucose

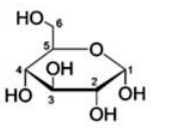

Original Substrate

3-methyl Glucose

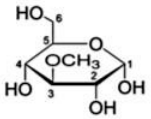

Substrate Analogue

If 3-methyl Glucose was added to Hexokinase, then it:

a. *might* induce Hexokinase to undergo a/the _____.
   A. same conformational change
   B. different conformational change
   C. same rate of conformational change
   D. None of the above

Achievement scores were obtained by simply counting the number of correct answers which are worth one point each. As for IE, we chose the formula $IE=\frac{Performance}{mental\ effort\ score}$ from a couple of mathematical formulas that appear in literature (Paas & van Merrie¨nboer, 1993, Kalyuga & Sweller, 2005). We used this formula as it is consistent with the general understanding of efficiency- an effect relative to spent resources needed to obtain a result (Kalyuga & Sweller, 2005). Obtained IE for the entire group is referenced to a critical level of efficiency defined as $IEcrit= Maximum\ Performance\ Score/Maximum\ Effort\ Score -$ ($\frac{5}{9}$ in our case) The rationale for using this critical level is based on the assumption that if a student spends maximum mental effort (9) to answer test questions but still does not ace the test (5), then his/her performance should not be considered as efficient (Kalyuga & Sweller, 2005).

Intervention

We conducted this study in a fairly large, public, research university. 30 college students participated in this research. Participants were from biology (43.3%), biochemistry (6.7%), and other (50%) majors that require at least a general biology course (medical technology, nursing, & nutrition). Number of college education years ranged from zero (freshman) to four (bachelor) with a mean of 2.47±1.59. After taking a pre-test, participants attended a lecture on substrate specificity of enzymes. Afterwards, they took the post-test followed by IMMS and a demographic survey.

As mentioned earlier, the lecture is based on a worksheet that consists of five experiments "segments." In the first experiment, students observe how the wild-type enzyme reacts to its natural substrates through changing its shape to get them aligned and close enough to react. The aim of this experiment is to explain the role of conformational change in aligning substrates thus speeding up the chemical reaction. To emphasize the role of catalytic amino acids in this process, the second experiment deals with a mutant form of the enzyme in which the reactive catalytic amino acid residue has been replaced by a non-reactive one. Students note that the enzyme would undergo the same conformational change as in the first experiment but still no reaction. The third set of experiments demonstrates the possible reactions of the enzyme toward substrate analogues. Students here notice how the enzyme reacts differently by undergoing an improper conformational change that fails to align the bound substrates along with the reactive amino acid. They also learn that, in few cases, the enzyme may react in an undesirable rate of conformational change. This helps students realize that enzyme specificity is a kinetic property of the enzyme; an objective that is covered in the last two experiments. In these final experiments, students learn that enzyme specificity mainly depends on kinetic parameters like binding affinity of substrates to their enzyme and reactivity of the enzyme toward these substrates. For binding affinity, students count the number of possible H-bonds that can form between a natural substrate and its surrounding catalytic amino acids. They do the same with a substrate analogue to examine which is more attracted to the enzyme, thus increasing the chances for the desired chemical reaction to take place. In the last experiment, the instructor demonstrates how the enzyme reacts with almost all of

the natural substrate molecules while reacting to very few of the analogue. The fact that the enzyme reacts with an analogue, though at a very low rate, helps students appreciate that enzyme specificity is more than a simple all-or-none phenomenon. Rather, and building on previous experiments, they come to the conclusion that enzyme specificity is a complex process that depends on a number of related variables: how (1) a conformational change facilitates (2) the interaction between the substrates and catalytic amino acids which in turn is directly connected to (3) the binding affinity of these substrates to these same amino acids as well as (4) the reactivity of the enzyme toward these substrates.

RESULTS AND REFLECTIONS

Reliability scores for the used instruments are summarized in Table.2. Cronbach α coefficient values for all of the instruments, including almost all of the subscales, were above 0.7. We also obtained face validity of the pre/post-test from five independent science educators who checked the clarity and validity of each item as it relates to the intended cognitive order "*Remember*" of Revised Bloom's taxonomy (Anderson et al., 2001).

Table 2

Reliability Scores of Used Instruments

	ECL		IMMS					Pre-test	Post-test
			Subscales				Entire Scale		
	Low	High	Attention	Relevance	Confidence	Satisfaction			
Score	**.784**	**.750**	.802	.696	.741	.794	**.895**	**.718**	**.711**

ECL= Essential Cognitive Load survey, IMMS= Instructional Material Motivation Survey

Interestingly, significant increases in test scores were shown from paired sample t-test indicating a successful intervention in terms of achievement, t(29)=- 4.164, p<.001 (Figure.3). Overall mental effort reported by students also revealed a reasonable outcome, 4.51±1.22. This level of mental effort lies between the two labels "4=slightly low" and "5=medium" in the survey which means that students perceived the lesson as neither too easy nor too demanding for them to understand. Group's mean IE was also higher than critical IE (IE>IEcrit; 0.79±.55 >0.55). This indicates that our intervention was efficient in helping students arrive at correct answers with relatively low mental effort (Kalyuga & Sweller, 2005).

Results obtained from IMMS scale also showed a high overall mean (4.20±.47) as well as high means in all of the constituting subscales, attention (4.38±.48), relevance (4.13±.63), confidence (3.99±.62), and satisfaction (4.22±.61) (Figure.4). Collectively, these results suggest that students were motivated to learn about enzyme specificity through using the presented instructional material. Specifically, this material helped them stay engaged in the learning process as they perceived it to be relevant, easy to use, and enjoyable.

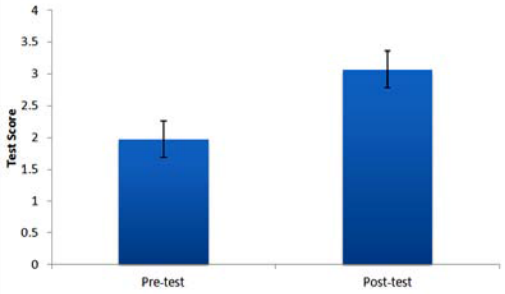

Figure 3: Achievement

Figure 4: Motivation

CONCLUSIONS AND FUTURE WORK

It might be challenging to mass communicate with textbook publishers referring to the inconsistency in representing enzyme specificity and its potential influence on the progress of tertiary biochemical education. Alternatively, we share this instructional material that we found motivating, effective, and cognitively efficient to learn about the concept. Our introduction of an interactive instructional model stands as a response to a call by the National Research Council in Next Generation Science Standards NGSS which emphasizes the important role of models in 21st century education. For instance, NGSS framework states that "models should increasingly be used across the grades, both in instruction and curriculum materials" (Schweingruber et al, 2012, p.59).

We mention two limitations in this study that are also guiding our future work. Although assessing students' retention of the learned material represents the foundation that higher levels of learning builds on, college level learning requires assessing intellectual behavior such as "Applying" an "Analyzing" (Zhao et al., 2014, Anderson et al., 2001). Accordingly, developing a transfer test would be good of an extension to the present study.

The fact that participants reported average mental effort, rather than low, might have arisen from the lack of prerequisite knowledge as 63.3% of participants reported not taking any prior biochemistry courses. In this scenario, some students would have experienced cognitive overload as they tried to simultaneously understand the scientific terms along with the explained process. To overcome this potential problem, a pre-training episode can be offered just before the session where students get to know the terms and discrete details related to enzymes (Mayer, 2009). An experimental approach would then be applied and effect sizes of the intervention can hence be determined.

REFERENCES

Anderson, L. W., Krathwohl, D. R., Airiasian, W., Cruikshank, K. A., Mayer, R. E., & Pintrich, P. R. (2001). A taxonomy for learning, teaching and assessing: A revision of Bloom's Taxonomy of educational outcomes: Complete edition.

Brewer, C. A., & Smith, D. (2011). Vision and change in undergraduate biology education: a call to action. American Association for the Advancement of Science, Washington, DC.

DeLeeuw, K. E., & Mayer, R. E. (2008). A comparison of three measures of cognitive load: Evidence for separable measures of intrinsic, extraneous, and germane load. Journal of Educational Psychology, 100, 223-234.

Fisher, E. (1894). Einfluss der Configuration auf die Wirkung der Enzyme: Berichte der Deutschen chemischen Gesellschaft zu Berlin, 27, 2985-2993.

Huang, W., Huang, W., Diefes-Dux, H., & Imbrie, P. K. (2006). A preliminary validation of Attention, Relevance, Confidence and Satisfaction model-based Instructional Material Motivational Survey in a computer-based tutorial setting. British Journal of Educational Technology, 37(2), 243-259.

Kalyuga, S., & Sweller, J. (2005). Rapid dynamic assessment of expertise to improve the efficiency of adaptive e-learning. Educational Technology Research and Development, 53(3), 83-93.

Keller, J. M. (1987). IMMS: Instructional materials motivation survey. Florida State University.

Kirschner, F., Paas, F., & Kirschner, P. A. (2009). Individual and group-based learning from complex cognitive tasks: Effects on retention and transfer efficiency. Computers in Human Behavior, 25(2), 306-314.

Koshland, D. E. (1958). Application of a Theory of Enzyme Specificity to Protein Synthesis: Proceedings of the National Academy of Sciences of the United States of America, 44(2), 98-104.

Lehman, S., Schraw, G., McCrudden, M. T., & Hartley, K. (2007). Processing and recall of seductive details in scientific text. Contemporary Educational Psychology, 32, 569–587.

Marcus, N., Cooper, M., & Sweller, J. (1996). Understanding instructions. Journal of educational psychology, 88(1), 49.

Mayer, R. E. (2009). Multimedia learning (2nd ed). New York: Cambridge University Press.

Paas, F., & Van Merriënboer, J. J. G. (1993). The efficiency of instructional conditions: An approach to combine mental effort and performance measures. Human Factors, 35, 737–743.

Pollock, E., Chandler, P., & Sweller, J. (2002). Assimilating complex information. Learning and instruction, 12(1), 61-86.

Saleh, M.R., Halverson, K., & Gearity, B. (2013, April 6-9). Moving Students to a Better Understanding of Enzyme Specificity. Paper presented at 2013 NARST Annual International Conference: The S in STEM Education: Policy, Research and Practice, Rio Grande, Puerto Rico.

Schönborn, K. J., & Anderson, T. R. (2006). The importance of visual literacy in the education of biochemists*. Biochemistry and molecular biology education, 34(2), 94-102.

Schweingruber, H., Keller, T., & Quinn, H. (Eds.). (2012). A Framework for K-12 Science Education: Practices, Crosscutting Concepts, and Core Ideas. National Academies Press.

Sweller, J., & Chandler, P. (1994). Why some material is difficult to learn. Cognition and instruction, 12(3), 185-233.

Van Gog, T., Paas, F., & van Merriënboer, J. J. (2008). Effects of studying sequences of process-oriented and product-oriented worked examples on troubleshooting transfer efficiency. Learning and Instruction, 18(3), 211-222.

Vekiri, I. (2002). What is the value of graphical displays in learning?. Educational Psychology Review, 14(3), 261-312.

Zhao, N., Wardeska, J.G., McGuire, S.Y., & Cook, E. (2014). Metacognition: An effective tool to promote success in college science teaching. Journal of College Science Teaching, 43(4), 48-54.

TRANSMISSION ELECTRON MICROSCOPY STUDY OF *Listeria monocytogenes* Serotype 1/2a CELLS EXPOSED TO SUBLETHAL HEAT STRESS AND CARVACROL

Sulagna Saha[1], Nitin Dhowlaghar[1], Amanda Lawrence[2], Ramakrishna Nannapaneni[1*], Chander S. Sharma[3], Barakat S.M. Mahmoud[1]

[1]Department of Food Science, Nutrition and Health Promotion, Mississippi State University, Mississippi State, MS 39762.
[2]Institute for Imaging and Analytical Technologies, Mississippi State University, MS 39762.
[3]Poultry Science Department, Mississippi State University, MS State, 39762.

[*]Author for correspondence: E-mail: nannapaneni@fsnhp.msstate.edu

ABSTRACT

The objective of this study was to investigate the morphological changes that occurred in *Listeria monocytogenes* serotype 1/2a cells as visualized by transmission electron microscopy (TEM) after exposure to sublethal heat stress at 48°C for 60 min and in combination with lethal concentration of carvacrol for 30 min. The morphological changes in *L. monocytogenes* were classified into changes occurring in the cell surface, cell wall, cell membrane and cytoplasm. The TEM micrographs revealed the thickening of cell wall and cell membrane, clumping of cytoplasm, loss of cytoplasm, pore formation and membrane bleb formation in *L. monocytogenes* cells when subjected to sublethal heat stress followed by carvacrol treatment. These findings indicate that *L. monocytogenes* cells when subjected to different stresses may alter their cellular morphology which may aid in their survival. Further studies will investigate the effect of increased contact time with carvacrol and with other essential oils on the ultrastructural changes in *L. monocytogenes* cells adapted to sublethal heat stress.

INTRODUCTION

Listeria monocytogenes is widely recognized as an important food borne pathogen responsible for nearly 25 to 30% of all fatalities from foodborne illnesses in the USA (Cartwright et al., 2013). Due to the zero tolerance requirements for *L. monocytogenes* in processed ready-to-eat foods, food industries are constantly devising novel strategies for its control in the food processing environments and in finished products. This pathogen is a major concern for food industries since it has the ability to survive a wide range of environmental stresses (Skandamis et al., 2008). Recently, screening of heat resistance (at 60°C/10 min) of 37 *L. monocytogenes* strains collected from various sources showed significant variation with some strains yielding 7 log reductions while others with as little as 2 log CFU/ml reductions (Shen et al., 2014). Previously, Linton et al. (1992) reported that the log phase cells of *L. monocytogenes* strain Scott A after heat shock at 48 °C for 10 min had 2.1-fold increase in $D_{55\ °C}$ value. Also, Fedio and Jackson (1989) found that the preheated *L. monocytogenes* Scott A at 48 °C for 1 h, and then heated at 60 °C, had a 3-4 log higher survival than control. Other studies show that *L. monocytogenes* was found to develop high tolerance to heat by undergoing changes in its growth, ultrastructure, surface properties, and intracellular structures. For example, Bermudez-Aguirre et al. (2011) determined the mechanisms of inactivation of *L. innocua* in thermally sonicated milk using transmission electron microscopy. Their findings show that thermal sonicating technology causes weakening of the cell by forming cavitation in the cellular structure and disruption and breakdown of cellular materials, formation of pores, lack or clumping of cellular material, breakdown of cell membrane, and inactivation of the target microorganism.

Food industries are continuously considering new cost-effective antimicrobial intervention technologies or treatments to achieve *L. monocytogenes* reduction. Essential oils are attracting considerable attention from the food industries due to their natural antifungal, antibacterial, and antioxidant effects (Burt, 2004). Phenolic constituent carvacrol is the major antimicrobial active ingredient in essential oils. However, recent findings show that heat stress adapted cells of *L. monocytogenes* has increased resistance to carvacrol (Ait-Ouazzou et al., 2012). Understanding the influence of heat stress adaptation on *L. monocytogenes* survival during treatment with carvacrol is very relevant for developing improved food preservation treatments. Since there is a potential occurrence of stress-resistant strains of *L. monocytogenes*, understanding their environmental stability and biocide resistance will be of immense significance (Holah et al., 2002). The objective of this study was to use transmission electron microscopy to investigate the morphological changes that occurred in *L. monocytogenes* serotype 1/2a cells after exposure to a

sublethal heat stress at 48°C and in combination with a lethal concentration of carvacrol.

MATERIALS AND METHODS

L. monocytogenes BUG 600 (EGD), serotype 1/2a was maintained at 4°C in slants of Tryptic soy agar supplemented with 0.6% of yeast extract (TSA-YE). Stationary phase culture was prepared by inoculating one loop of working stock culture in 10 ml of TSB-YE and incubated at 37°C for 24 h to obtain cell concentration of ~10^9 CFU/ml using an incubator shaker (C24 classic series, New Brunswick Scientific, Edison, NJ). Carvacrol was purchased from Sigma Aldrich (St. Louis, MO) and solubilized by diluting (1:1) into propylene glycol (PG) and a concentration of 428 ppm was prepared in TSB-YE. For sublethal heat adaptation, 1 ml of stationary phase culture was diluted to 9 ml of TSB-YE to obtain 10^8 log CFU/ml and exposed to 48°C for 60 minutes using a water bath (Reciprocal water bath shaker, model R76, New Brunswick Scientific, Inc., Edison, NJ, USA), while the control non-adapted cells of *L. monocytogenes* were kept at room temperature for 60 minutes. Then sublethal heat-adapted and non-adapted *L. monocytogenes* cells were exposed to a lethal concentration of carvacrol (428 ppm) for 30 minutes at room temperature (22°C). The samples were centrifuged at 12,000 x g for 5 min to remove carvacrol and the resulting concentrated cell pellets were prepared for transmission electron microscopy (TEM) using the methods described previously (Capita et al., 2014). Pellets were fixed in 2.5% glutaraldehyde in 0.1M sodium cacodylate buffer (pH 7.2) overnight at 4°C. Pellets were post fixed in 2% buffered (0.1M sodium cacodylate) osmium tetroxide, dehydrated through a graded ethanol series, and embedded in Spurr's resin. Ultra-thin sections were stained with uranyl acetate and lead citrate then viewed on a JEOL JSM-1230 transmission electron microscope at 80kv.

RESULTS AND DISCUSSION

Previous findings show that *L. monocytogenes* cells when exposed to sublethal heat stress may survive lethal heat treatments. For example, the 1983 outbreak of listeriosis in Massachusetts was epidemiologically linked to a high-temperature short-time (HTST) pasteurized milk (Bunning et al., 1992). In this case, when *L. monocytogenes* cells were shifted from a lower to higher temperature within a short period, it caused an acquired thermotolerance or protection against lethal temperature (Bunning et al., 1992). Similarly, the thermal resistance of *L. monocytogenes* was observed in meat with pre-heat shocked cells of 48 °C for 2 h which exhibited a 2.4 fold increase in the $D_{64°C}$ value (Farber and brown, 1990). In this present study, we have used transmission electron microscopy to investigate the morphological changes that occurred in *L. monocytogenes* serotype 1/2a cells after exposure to a sublethal heat stress at 48°C and in combination with a lethal concentration of carvacrol.

The presence or absence of various morphological changes in *L. monocytogenes* serotype 1/2a cells when exposed to sublethal heat stress alone or in combination with lethal concentration of carvacrol are summarized in Table 1. These morphological changes in *L. monocytogenes* were classified into changes occurring in the cell surface, cell wall, cell membrane and cytoplasm. *L. monocytogenes* serotype 1/2a cells when exposed to sublethal heat stress at 48°C for 60 min showed several cellular changes as compared to that of non-heat stressed cells. Two distinct morphological changes in *L. monocytogenes* cells after exposure to sublethal heat stress were the thickening of cell wall and clumping of cytoplasm with some exceptions as compared to that of non-heat shocked control cells (Figure 1). About 81% of the cells had thickening of the cell wall after sublethal heat stress. In the presence of lethal concentration of carvacrol, *L. monocytogenes* cells exhibited significant morphological changes including coccid cell formation, clumping of cytoplasm or leakage of cytoplasmic contents through pore formation and membrane bleb formation (Figure 2). *L. monocytogenes* serotype 1/2a cells after exposure to sublethal heat stress at 48°C for 60 min followed by lethal treatment with carvacrol at 428 ppm/30 min exhibited thickening of cell walls and appearance of a rough texture of cell wall. Other significant morphological changes in *L. monocytogenes* include cellular disintegration, pore formation, membrane bleb formation and clumping of cytoplasm (Figure 3). Under these treatments, nearly 86% of the cells had thickening of cell wall and 6% of the cells exhibited pore formation. Ait-Ouazzou et al. (2011) were the first to observe the damage in cell envelopes by carvacrol. Their studies proposed that microbial inactivation occurred as a result of damage by carvacrol that first took place in the outer membrane of the cell then later on the cytoplasm. Cross resistance to carvacrol resulted in the alteration of fatty acid composition and induction of heat shock proteins. Their findings also show that the sublethal heat shocked cells of *L. monocytogenes* exhibited higher survival by 3.0 log CFU/ml in the presence of carvacrol compared to that of non-heat shocked control cells (Ait-Ouazzou et al., 2012). In our experiments, there was about 2.5 log increase in the viable cell counts of *L. monocytogenes* serotype 1/2a cells in a lethal concentration of carvacrol (428 ppm for 30 min) when cells were pre-exposed to sublethal heat stress of 48 °C for 60 min (data not shown).

Table 1.

Summary of morphological changes in *L. monocytogenes* serotype 1/2a cells when exposed to sublethal heat stress and in combination with lethal concentration of carvacrol.

Changes in cell morphology of *L. monocytogenes* cells	TEM treatments of *L. monocytogenes* cells			
	37°C/60 min (Control)	37°C/60 min + 30 min carvacrol	48°C/60 min (Control)	48°C/60 min + 30 min carvacrol
Pore formation				
Loss of cell wall	-*	-	-	+
Disruption of cell membrane	-	+	-	+
Lack of cell membrane	-	+	-	+
Cell wall thickening	-	-	+	+
Membrane bleb	-	+	-	+
Filamentous membrane	-	+	-	-
Damage to cell surface	-	-	-	+
Cell wall thinning	-	-	-	+
Blurry cell wall	-	-	+	+
Cavity formation	-	-	+	-
Cell wall roughness	-	-	+	+
Cell division	+	+	+	+
Cytoplasmic clumping	-	+	+	+
Disorganization of cytoplasm	-	-	-	+
Lack of cytoplasm	-	+	+	+

*Presence (+) or absence (-) of cellular morphological changes in *L. monocytogenes*.

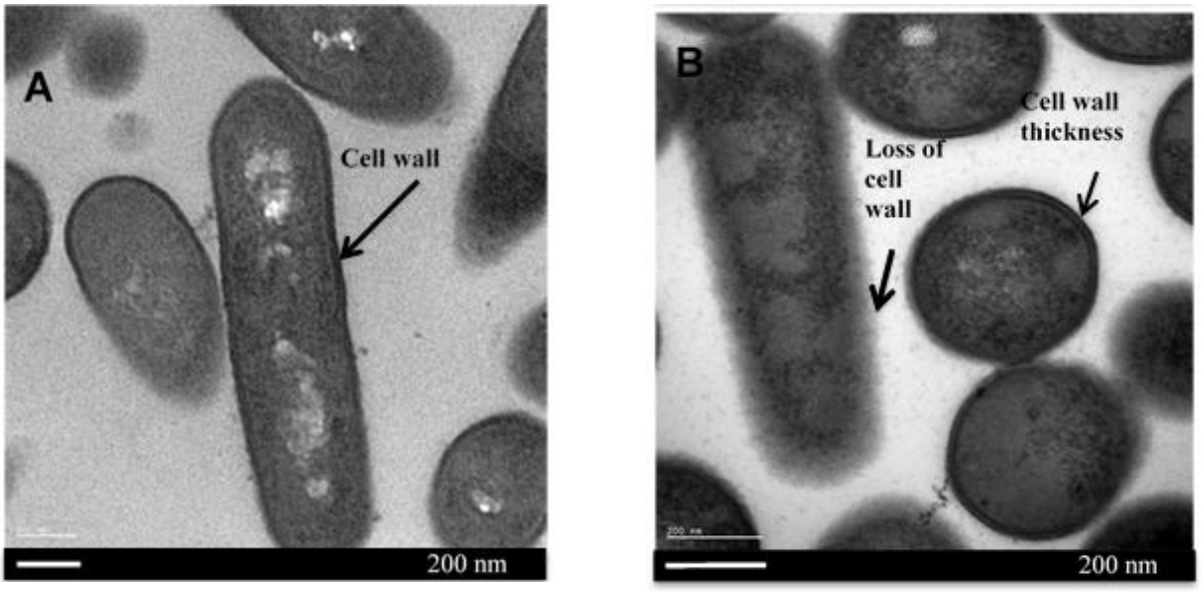

Figure 1. Transmission electron micrograph of *Listeria monocytogenes* serotype 1/2a: (A) untreated control cells; and (B) cells after exposure to sublethal heat stress at 48°C for 60 min. Control *L. monocytogenes* cells grown at 37°C have an intact cell wall. There is a loss of cell wall in some cases or there is a thickening of cell wall in other cases in *L. monocytogenes* serotype 1/2a after exposure to 48°C for 60 min.

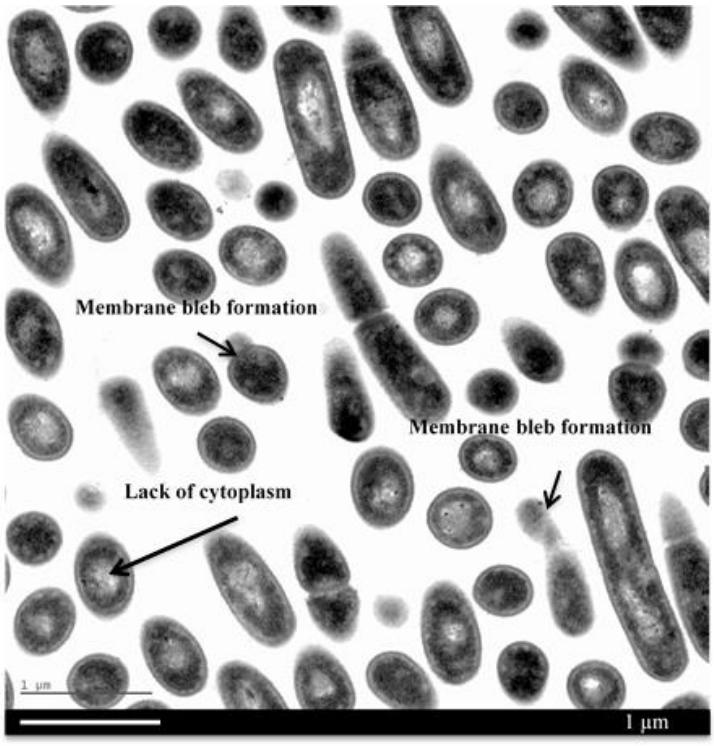

Figure 2. Transmission electron micrograph of *Listeria monocytogenes* serotype 1/2a cells after exposure to 428 ppm of carvacrol for 30 min at room temperature. These cells show clumping of cytoplasm or lack of cytoplasm or membrane bleb formation.

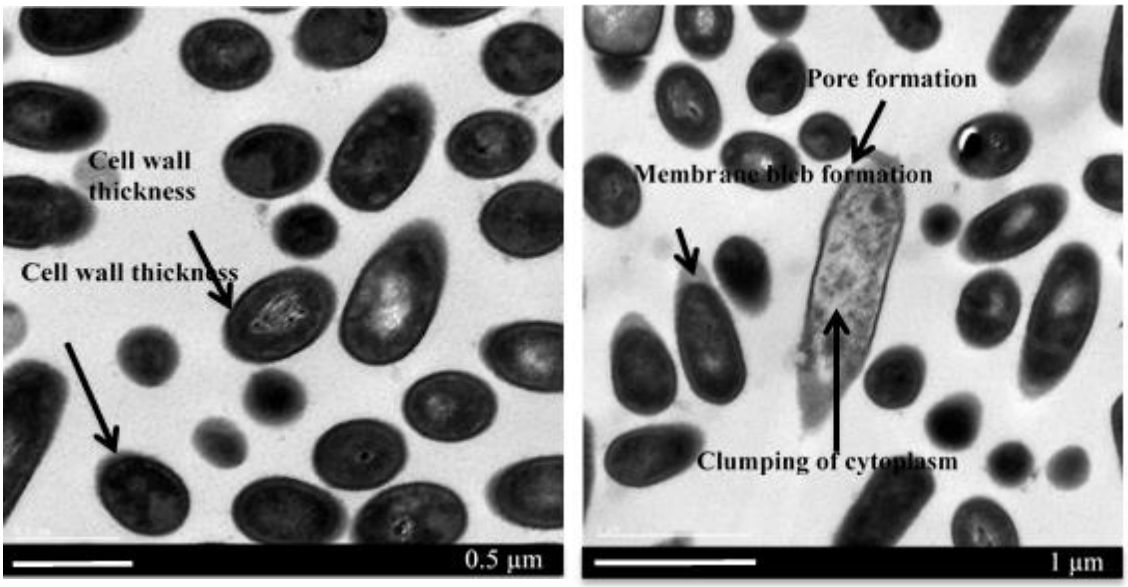

.

Figure 3. Transmission electron micrograph of *Listeria monocytogenes* serotype 1/2a cells after exposure to sublethal heat stress at 48°C for 60 min and then exposed to 428 ppm of carvacrol for 30 min at room temperature. These cells show thickening of cell wall, pore formation, membrane bleb formation, loss of cytoplasm and clumping of cytoplasm.

Previous studies using atomic force microscopy on *Bacillus cereus* revealed that carvacrol targets and disintegrates the cell envelope (Nostro and Papalia, 2012). These studies also demonstrated that carvacrol led to decreased cell length, size, and diameter. The mechanism of inactivation by carvacrol can be directly linked to the cell envelope and ability of carvacrol to permeabilize and depolarize the cell membrane (Ultee et al., 2002).

Perhaps the mode of inactivation by carvacrol can be attributed to a variety of factors such as pH of treatment medium, type of microbial specimen, and presence of outer membrane. Previous studies demonstrated that microbial inactivation took place at lower pH due to the chemical properties of carvacrol and that structural change by carvacrol were varied based on the pH of the treatment medium. These findings demonstrated that modifications in the outer membrane were shown to play a significant role in the adaptive response of bacteria to antimicrobial agents (Ernst et al., 2001; Sallum and Chen, 2008). It can also be suggested that bacterial cells might undergo certain chemical modifications such as changes in cellular hydrophobicity to repel water-soluble compounds as an adaptive mechanism (Capita et al., 2014). In conclusion, this study revealed the changes in cell morphology of *L. monocytogenes* serotype 1/2a cells when exposed to sublethal heat stress alone or in combination with lethal concentration of carvacrol that may play a role in its survival under these stress conditions.

ACKNOWLEDGEMENTS

This research was supported in part by the Food Safety Initiative awards to RN by the Mississippi Agricultural and Forestry Experiment Station (MAFES) under project MIS-401160. USDA-ARS SCA No. 58-6402-2729 contributed funding for this Food Safety Initiative project. Approved for publication as a journal article, number J-12738 of the Mississippi Agricultural and Forestry Experiment Station, Mississippi State University.

LITERATURE CITED

Ait-Ouazzou AA, Cherrat L, Espina L, Lora´n S, Rota C, and Paga´n R. 2011. The antimicrobial activity of hydrophobic essential oil constituents acting alone or in combined processes of food preservation. Innovative Food Science Emerging Technology 12: 320–329.

Ait-Ouazzou AA, Espina L, Gelaw TK, Castellvi SDL, Pagan R, and Gonzalo DG. 2012. New insights in mechanisms of bacterial inactivation by carvacrol. Journal of Applied Microbiology 114: 173-185.

Bermúdez-Aguirre D, Mawson R, Barbosa-Cánovas GV. 2011. Study of possible mechanisms of inactivation of *Listeria innocua* in thermo-sonicated milk using scanning electron microscopy and transmission electron microscopy. Journal of Food Processing and Preservation 35:767-77.

Bunning VK, Crawford RG, Tierney JT, Peeler JT. 1992. Thermotolerance of heat-shocked *Listeria monocytogenes* in milk exposed to high-temperature, short-time pasteurization. Applied and Environmental Microbiology 58: 2096-2098

Burt S. 2004. Essential oils: their antibacterial properties and potential applications in foods—a review. International Journal of Food Microbiology 94:223-53.

Capita R, Riesco-Peláez F, Alonso-Hernando A, Alonso-Calleja C. 2014. Exposure of *Escherichia coli* ATCC 12806 to sublethal concentrations of food-grade biocides influences its ability to form biofilm, resistance to antimicrobials, and ultrastructure. Applied and Environmental Microbiology 80:1268-80.

Cartwright EJ, Jackson KA, Johnson SD, Graves LM, Silk BJ, Mahon BE. 2013. Listeriosis outbreaks and associated food vehicles, United States, 1998–2008. Emerging Infectious Diseases 19: 1-9.

Ernst RK, Guina T, Miller SI. 2001. *Salmonella typhimurium* outer membrane remodeling: role in resistance to host innate immunity. Microbes and Infection 3: 1327-34.

Fedio WM, Jackson H. 1989. Effect of tempering on the heat resistance of *Listeria monocytogenes*. Letters in applied Microbiology 9: 157-160.

Farber JM, Brown BE. 1990. Effect of prior heat shock on heat resistance of *Listeria monocytogenes* in meat. Applied and Environmental Microbiology. 56: 1584-1587.

Holah J, Taylor J, Dawson D, Hall K. 2002. Biocide use in the food industry and the disinfectant resistance of persistent strains of *Listeria monocytogenes* and *Escherichia coli*. Journal of Applied Microbiology 92: 111S-20S.

Linton RH, Webster JB, Pierson MD, Bishop JR, Hackney CR. 1990. The effect of sublethal shock and growth atmosphere on the heat resistance of *Listeria monocytogenes* ScottA. J Food Prot. 55: 84-87.

Nostro A, Papalia T. 2012. Antimicrobial activity of carvacrol: current progress and future prospectives. Recent patents on anti-infective drug discovery 7: 28-35.

Shen Q, Jangam PM, Soni KA, Nannapaneni R, Schilling W, Silva JL. 2014. Low, medium, and high heat tolerant strains of *Listeria monocytogenes* and increased heat stress resistance after exposure to sublethal heat. J Food Prot. 77:1298-307.

Skandamis PN, Yoon Y, Stopforth JD, Kendall PA, Sofos JN. 2008. Heat and acid tolerance of *Listeria monocytogenes* after exposure to single and multiple sublethal stresses. Food microbiology 25:294-303.

Sallum UW, Chen TT. 2008. Inducible resistance of fish bacterial pathogens to the antimicrobial peptide cecropin B. Antimicrobial Agents and Chemotherapy 52:3006-12.

Ultee A, Bennik M, Moezelaar R. 2002. The phenolic hydroxyl group of carvacrol is essential for action against the food-borne pathogen Bacillus cereus. Applied and Environmental Microbiology 68: 1561-8.

PRELIMINARY STUDY OF BOTTLENOSE DOLPHIN (*Tursiops truncatus*) FORAGING BEHAVIOR ASSOCIATED WITH SHRIMP TRAWLS AND BY-CATCH DISPOSAL IN THE MISSISSIPPI SOUND

Siegel, Jeffrey[1]; Detweiler, Kelsey[2]; Breeden, Stephanie[3]; West, Anna[4]; Clark, Julia[4]; Kirby, Aaryn[5]; Mohr, Paige[6]; Ware, Alexandra[7]; Worsham, Rebecca[8]; Bean, Jordan[3]

[1]Mississippi Gulf Coast Community College, 2226 Switzer Road, Gulfport, MS 39507, USA
[2]Central Michigan University, 1200 South Franklin Street Mount Pleasant, MI, 48858, USA
[3]Tennessee Wesleyan College, 204 E. College Street, Athens, TN, 37303
[4]Westminster College, 501 Westminster Avenue, Fulton, MO, 65251, USA
[5]College of Charleston, 66 George Street, Charleston, SC, 29424, USA
[6]Iowa State University, Ames, IA, 50011, USA
[7]University of Southern Mississippi, 118 College Drive, Hattiesburg, MS, 39406, USA
[8]Mississippi State University Mississippi State University, Mississippi State, MS 39762

ABSTRACT

This project quantified bottlenose dolphin (*Tursiops truncatus*) behavior while dolphins foraged from commercial shrimp trawl nets or from by-catch tossed overboard from shrimp trawl vessels in the Mississippi Sound, USA. Any incident of injury or death to a dolphin resulting from such dolphin foraging behavior was documented.

Dolphin foraging behavior was observed from 3 different shrimp trawl vessels. Observations were conducted during 24 non-consecutive days coinciding with the onset of each of 4 years commercial shrimp harvesting seasons, 6 days in mid-May 2011-2014. Dolphins demonstrated significant boat approach behavior toward shrimp boats more so than other boats ($p < 0.05$). Dolphins were observed foraging from trawl nets and staying in close proximity to the stern of vessels while by-catch was separated and tossed overboard. No evidence of human-induced mortality or injury was observed during these interactions between dolphins and shrimp trawl gear or vessels.

INTRODUCTION

The United States National Oceanic and Atmospheric Administration (NOAA) recently elevated the Southeast Atlantic shrimp trawl fishery from "Category III" to a "Category II" enabling stricter federal shrimp trawl regulation (Greenman 2012). Any activity causing a change in dolphin migration, breathing, nursing, breeding, or feeding behavior is classified as "Level B Harassment" by NOAA and subject to federal regulation.

Commercial trawling fisheries of the Gulf of Mexico (GOM), including the Mississippi Sound, and east coast of the United States discard large amounts of by-catch which benefit bottlenose dolphins foraging these fish (Wassenberg and Hill 1990). Sounds created by human trawling activity may attract dolphins to specific sites and boats where by-catch may be discarded overboard allowing dolphins to forage. Leatherwood (1975) suggested that dolphins may have learned to acoustically differentiate between boats that are cruising and shrimp boats that are trawling.

This project took advantage of the naturally occurring foraging behavior of bottlenose dolphins described by Svane (2005) associated with by-catch disposal from commercial shrimp trawl practices in the Mississippi Sound. This study measured the amount of time it took bottlenose dolphins (*Tursiops truncatus*) to arrive near a shrimp trawl vessel whether or not a trawl net was deployed and the amount of time after a trawl net was deployed before dolphins engaged in foraging from the trawl net. The foraging behavior of mother-calf pairs was compared with the foraging behavior of other dolphins while foraging from shrimp trawl nets, including foraging behavior from by-catch after it was tossed overboard from shrimp trawl vessels.

METHODS

This study took place in Mississippi coastal waters of the northern Gulf of Mexico (GOM) near Ocean Springs and Point Cadet, Biloxi to the north, including the waters west of Deer Island, east to Pascagoula, and extending south of Horn Island twenty nautical miles. Three steel-hulled vessels were used to conduct trawls and observe dolphin behavior: a single screw, 21-ton, 11.64-meter (38.2-foot) long, 4.33-meter (14.2-foot) wide trawler with a 20.4-meter (6.7-foot) draft equipped to pull a standard 4.88-meter (16-foot) shrimp trawl net from the vessel's stern; a twin screw 35-ton, 16.76-meter (55-foot) long, 4.63-meter

(15.2-foot) wide trawler with a 1.71-meter (5.6-foot) draft equipped to pull a standard 4.88-meter (16-foot) shrimp trawl net from the vessel's stern; and the third vessel was a twin screw, 158-ton, 26.39-meter (86.6-foot) long, 7.62-meter (25-foot) wide trawler with a 3.08-meter (10.1-foot) draft equipped to pull a standard 12.80-meter (42-foot) shrimp trawl net from the vessel's stern.

Observational periods of 35-minutes included a 10-minute pre-trawl period to locate any dolphins that might be in the area, classify the dolphins' behavioral states, followed by lowering the trawl net into the water, dragging it 150 meters behind the vessel for 10 minutes, and then hoisting the trawl net aboard the vessel to separate by-catch.

By-catch was quickly separated from shrimp and assorted into buckets of discrete fish species. Except for the grouping of by-catch by species in order to detect fish preference behavior among the dolphins, by-catch was discarded in a manner similar to other commercial shrimp trawl vessels. Buckets, each containing an equal amount but different species of by-catch, were simultaneously emptied from the vessel's stern so that discrete accumulations of by-catch species occurred in the water and observers could note which species of fish the dolphins ate first when multiple species were available.

Observations were conducted during 24 non-consecutive days coinciding with the onset of each of 4 years commercial shrimp harvesting seasons, 6 days in May 2011, 6 days in May 2012, 6 days in May 2013, and 6 days in May 2014. A minimum of 4 trawls were pulled each of the 24-days, with at least 2 in the morning and 2 in the afternoon. Up to 18 observers stationed at various places aboard each vessel classified and documented the dolphins' behavioral states such as traveling, foraging, socializing, or resting before each trawl (Mann et al 2000); behavioral events such as boat avoidance, boat approach, diving on the shrimp net, and milling near the vessel's stern (Mattson et al 2005) was documented both during and after trawls at 5-minute intervals. Aggressive and competitive behavior between dolphins such as tooth raking, biting, jaw popping, ramming, and hitting (Holobinko and Waring 2010) were also documented at 5-minute intervals during observational periods. Both behavioral states and events were coded onto ethograms, sheets of paper for tabulating the observed occurrences of each behavior. Behavioral states were coded as either occurring or not during each time interval, zero-one sampling; while the total number of each behavioral event per time increment was tabulated. Dolphins were visually inspected and photographed from the vessels to detect any indications of human-induced mortality or injury as defined by Read and Murray (2000).

The behavioral data from ethograms was electronically collated and collectively analyzed using IBM SPSS (2013) statistical package which was used to generate the Pearson product moment coefficient of correlation statistics presented in the results.

RESULTS

A total of 83 trawls were conducted, with 42 trawls from the smaller vessel, 29 trawls from the medium sized vessel, and 12 trawls from the larger vessel. Dolphins were likely to change their behavioral state and approach a trawl net within 5 minutes of its deployment ($r=0.70$, $p = 0.01$). No boat avoidance behavior was observed during times just prior to or during shrimp trawling. Dolphin boat approach behavior was not found to be significant before the trawl net was deployed and during times when no shrimp trawling occurred. On one occasion, dolphins approached the vessel moments before the net was lowered into the water.

When the research vessel was idle and drifting both before and after trawling, a decrease in dolphin traveling with a corresponding increase in dolphin socialization near the research vessel was observed ($r = 0.68$, $p = 0.01$). When the research vessels were traveling slowly but not engaged in shrimp trawling, dolphins were observed traveling in small groups ($r = 0.78$, $P = 0.01$). After a shrimp trawl was deployed, large groups of dolphins were observed converging on the trawl ($r = 0.71$, $p = 0.01$).

During by-catch disposal, dolphins frequently approached within a meter from the stern of the vessel where by-catch was tossed overboard. They would remain within close proximity of the vessel for as long as by-catch was tossed overboard. When by-catch disposal ceased, dolphins were observed dispersing in small groups from the vessel.

Mother-calf pairs were observed diving on the shrimp trawl nets ($r = 0.84$, $p = 0.01$) while maintaining a greater distance from the stern of the trawl boat than other dolphins. Adults without calves as well as juveniles were seen within 5 meters from the stern of the trawl boats when by-catch was tossed overboard ($r = 1$, $p = 0.01$), but mother-calf pairs were not observed foraging by-catch at the stern of the vessels.

The most prevalent by-catch species were pogi (*Brevoortia patronus),* cutlass fish *(Assurger anzac),* white trout *(Paralichtys albigutta),* Atlantic menhaden *(Brevoortia tyrannus),* croaker *(Micropognias undulates),* spot *(Cynoscion arenarius),* and mantis shrimp *(Leiostomus xanthurus)*. Observations of fish preference by dolphins foraging from the by-catch indicated cutlass fish, white trout, and spot were preferred over croaker, menhaden, and pogi. When buckets, each containing an equal amount but different species of by-catch, were simultaneously emptied overboard, dolphins would pass

up fish closer to them such as croaker and pogi to compete with other dolphins for cutlass fish, white trout, and spot. When menhaden, croaker, and pogi were available, dolphins were observed to first grab menhaden until it was unavailable, then pogi. Croaker were left uneaten indicating this may be the least desirable by-catch species. During these observations of foraging from by-catch, dolphins were frequently observed engaging in aggressive competitive behavior indicated by thrashing their tail toward other dolphins, raking other dolphins with their teeth, and chuffing underwater creating large bubble rings.

Although dolphins, including mothers with young calves, were observed interacting with shrimp trawl nets by diving on the nets and leaving tooth marks on the net, and swimming in close proximity to the stern of vessels as by-catch was tossed overboard, no dolphin was observed to have been injured or killed while engaging in foraging behavior during this study.

DISCUSSION

In this preliminary study, dolphins were observed interacting with trawl gear used by commercial shrimp trawlers. The presence of trawling activity altered dolphin behavior meeting the NOAA criteria of "Level B Harassment" as indicated by dolphins changing their behavioral state in order to follow a trawl. However, trawling did not appear to distress the dolphins but appeared to be a benefit to them. In conclusion, the NOAA definition of "Level B Harassment" may need continued scrutiny as dolphins may resort to foraging from commercial fishing vessels as a strategy to reduce overall foraging effort or compete against human over-fishing or other anthropogenic or natural factors that may disrupt the dolphins' ability to find food or alter their food supply. More research is necessary to characterize the association of dolphins with commercial shrimp fisheries in different regions of the GOM as generally either harmful or beneficial to dolphin populations or individuals.

ACKNOWLEDGEMENTS

The authors thank Dr. Jeffrey Lotz and Sam Clardy of the University of Southern Mississippi Gulf Coast Research Laboratory (USM-GCRL). Captain Larry Bosarge USM-GCRL R/V Hermes, and Captain R. Block, Jr. USM-GCRL R/V Tommy Munro and R/V Tom McIlwain, and the crews of the USM-GCRL research vessels. The authors also thank Dr. Kelly Rouse and Joyce Shaw for their assistance reviewing the manuscript.

LITERATURE CITED

Greenman, J. 2012. A Characterization of Bottlenose Dolphin (*Tursiops truncatus*) interactions with the commercial shrimp trawl fishery of South Carolina. *M.S. Thesis*. College of Charleston, Charleston, South Carolina. 114 pp.

Wassenberg T. J., and B. J. Hill. 1990. Partitioning of material discarded from prawn trawlers in

Moreton Bay. Australia Journal of Marine and Freshwater Research 41:27-36.

Leatherwood, S. 1975. Some observations of feeding behavior of bottle-nosed dolphins (*Tursiops truncatus*) in the Northern Gulf of Mexico and (*Tursiops* cf. *T. gilli*) off Southern California, Baja California, and Nayarit, Mexico. Marine Fisheries Review 37(9), 10-16.

Svane, I. 2005. Occurrence of dolphins and seabirds and their consumption of by-catch during prawn trawling in Spencer Gulf, Australia. Fisheries Research 76(3), 317-327.

Mann, J., et al Cetacean Societies: Field Studies of Dolphins and Whales. Chicago: University of Chicago Press, 2000. 435 pages.

Mattson, M. C., J. A. Thomas, and D. St. Aubin. 2005. Effects of boat activity on the behavior of bottlenose dolphins (*Tursiops truncatus*) in waters surrounding Hilton Head Island, South Carolina. Aquatic Mammals 31(1), 133-140.

Holobinko, A. and G. H. Waring. 2010. Conflict and reconciliation behavior trends of bottlenose dolphin (*Tursiops truncatus*). Zoo Biology 29(5), 567-585.

Read, R. J. and K. T. Murray. 2000. Gross evidence of human-induced mortality in small Cetaceans. NOAA Technical Memorandum NMFS-OPR-15. 21 pages.

IBM Corp. Released 2013. IBM SPSS Statistics for Windows, Version 22.0. Armonk, NY: IBM Corp.

THE OCCURRENCE OF THE GREEN ALGAL LEAF ENDOPHYTE *STOMATOCHROON* (TRENTEPOHLIALES) IN MISSISSIPPI

Daniel E. Wujek
Department of Biology, Central Michigan University, Mt. Pleasant, MI 48859
Wujek1de@cmich.edu

ABSTRACT

The green endophytic alga *Stomatochroon* is reported from Mississippi for the first time. This paper represents its second report for North America.

Keywords: Stomatochroon, Trentepohliales, leaf parasite

.

INTRODUCTION

The green algal order Trentepohliales (Chlorophyta) consists of a single family, the Trentepohliaceae, with six genera. These algae are not aquatic, but rather subaerial, growing on humid soil, rocks, buildings, tree bark, leaves, stems, fruit and a few select mammals. Some species are endophytic or parasitic, whereas others grow in close association with fungi, forming lichens (Chapman and Good, 1983a, b; Chapman and Waters, 2002). The cells are uni- or multinucleate, with several parietal chloroplasts that can be discoid or band-shaped, sometimes appearing reticulate. Most trentepohlialean genera develop a filamentous thallus that forms either uniseriated, branched, erect tufts or laterally coherent, prostrate discs. Others are highly reduced and produce only a short vegetative filament a few cells in length. Reproduction occurs by asexual quadriflagellate zoospores or sexual biflagellate gametes (Bourrelly, 1966; Chapman, 1984; Silva, 1982; Sluiman, 1989; O'Kelly and Floyd, 1990; Thompson and Wujek, 1997).

The main characteristics that distinguish members of the order Trentepohliales from other green chlorophycean algae are as follows: differentiated reproductive cells; the presence of ß-carotene and haematochrome (i.e., astaxanthin), which color the algal thallus yellow, orange, or red; the absence of a pyrenoid in the chloroplasts; unique flagellar apparatus; and transverse cell walls with plasmodesmata.

Cephaleuros is probably the best known genus of the order Trentepohliales. It causes red rust disease in some important economic plants in the tropics (Nelson 2008; Ponmurugan et al., 2010; Ramya et al., 2013, Brooks, 2014; Brooks et al., 2015). *Stomatochroon* is known to infect land plants but it has been far less studied. It the only genus in the order known to parasitize the hosts mesophyll. All other trentepohlian genera occupy space on the surface of the substratum or if on a leaf, either on the cuticle or between the cuticle and epidermal layer.

Stomatochroon lagerheimii B.T. Palm was described in 1934 (Palm 1934). Thompson and Wujek (1997) emended the description and described three additional species: *Stomatochroon coalitus*, *S. consociatus*, and *S. reniformis*. A new variety of *S. reniformis*, var. *chinensis*, from south China was recently described (Zhu et al., 2014). All of these taxas grow endophytically in the substomatal chambers and through the intercellular spaces (mesophyll) of vascular plant host leaves (López-Bautista et al., 2002). *Stomatochroon*'s life history consists of an alternation of heteromorphic generations (Thompson and Wujek, 1997). The sporophyte is a multicellular thallus typically consisting of internal (i.e. within the host tissue) branched filaments or a single anchoring cell and external structures (usually consisting of a sterile hair and one or more clavate cells). The sporangiate-laterals are produced on clavate cells. The internal and external systems are connected by a basal cell in the substomatal chamber. The gametophyte consists of unicellular sterile hairs and lateral gametangia.

In this study, I report on collections of *Stomatochroon consociatus* from southern Mississippi. It the second report of this genus in North America. A TEM image of a gametangium is also illustrated.

MATERIALS AND METHODS

Stomatochroon consociatus samples were collected from *Vibernum odoratissimum* and along I-10 in Hancock and Harrison Counties, Mississippi. Leaves colonized by *Stomatochroon* were cut into small squares and fixed with 2% buffered glutaraldehyde for one hour at room temperature. The squares were dehydrated through an acetone series, 15 min per step. Some squares were critical-point dried, mounted on stubs, coated with gold for 30 s, and observed with a JEOL 840-A SEM. Other

squares were post-fixed in buffered 1% OsO_4 for one hour and embedded in mixture number one of Epon-Araldite (Mollenhauer, 1964). TEM sections were observed in a Philips EM300. In December, 2014, Stone County, a second host, *Magnolia grandiflora* was also observed infected with *Stomatochroon*.

RESULTS AND DISCUSSION

Stomatochroon consociatus Thompson and Wujek was first reported in North America growing on leaves of *Vibernum odoratissimum* on the campus of Louisiana State University, Baton Rouge (Timpano and Pearlmutter, 1983). I first observed it growing epiphytically and endophytically on the leaves of two different flowering vascular plants, *Magnolia* and *Vibernum*, along the I-10 corridor in Hancock County, Mississippi. There they were producing necrosis of the mesophyll of leaves along with the production of both asexual and sexual reproductive structures (Figures 1-4). I observed it most recently, December, 2014, growing in Hancock and Harrison Counties.

It occurs predominantly at drip points of the leaf but sometimes along the midrib and occasionally on wide areas of the leaf. Unlike damage caused by *Cephaleuros* spp whose thallus produces a "red-rust" on the adaxial (upper) surface of leave, the necrotic leaf regions caused by *S. consociatus* were present only on abaxial surfaces (underside) of leaves (Fig. 1). Also present on the lower epidermis were clusters of gametangia (Figs. 2-3) and one TEM of a gametangium prior to gamete release (Fig. 4).

Stomatochroon taxa are restricted to leaves of angiosperms differing from other genera in the family which grow on various other plant organs, in free-living states, and even observed as phycobiont partners in lichens (López-Bautista et al., 2002). Studies are needed to define the interaction of the alga with their hosts. Thompson (unpublished) has even suggested that they may cause host leaves to become waterlogged and subject to sun scald. As Timpano and Pearlmutter (1983) have stated "there are indications that *Stomatochroon* is the most widely distributed genus of the Trentepohliaceae yet it is the least studied." To date no molecular studies have been conducted to show relationships between species in the genus let alone to other members of the trentepohlian family.

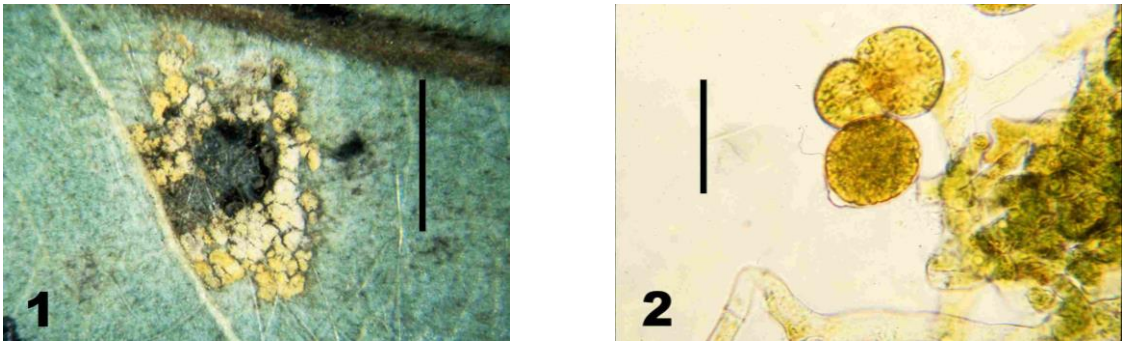

Figs. 1-2. *Stomatochroon consociatus*. 1. Stereoscope image of a lesion on a *Vibernum* sp. leaf. 2. SEM of gametangia. Scale bar: 1 = 25 cm, 2 = 15 µm

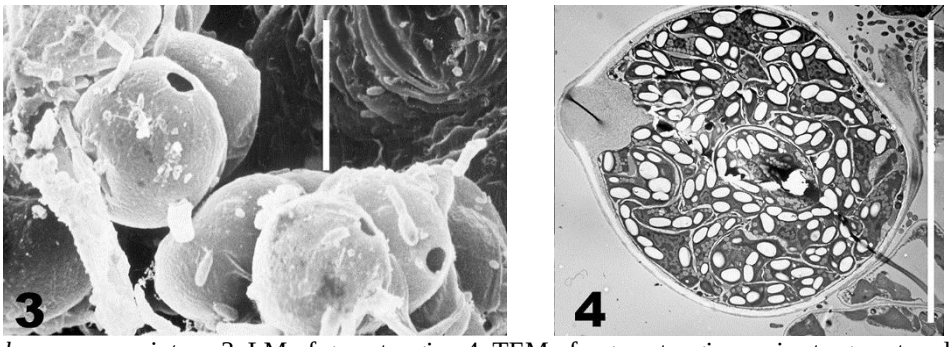

Figs. 3-4. *Stomatochroon consociatus*. 3. LM of gametangia. 4. TEM of a gametangium prior to gamete release. Scale bar = 25 µm

ACKNOWLEDGEMENTS

I thank M. Wujek for field assistance and B. Roberts for help in the preparation of the figures.

LITERATURE CITED

Bourrelly, P. 1966. Les algues d'eau. I. Les algues vertes. N. Boubee, Paris, 511 pp.Brooks, F. 2014 Plant parasitic algae (Trentepohliales, Chlorophyta) in American Samoa. Pacific Science. 58:419-428.

Brooks, F, Rindi F, Suto, Y, Ohtani S, Green M. 2015. The Trentepohliales (Ulvophyceae), Chlorophyta): an unusual order and its novel plant pathogen, *Cephaleuros*. Plant Disease 99: 740-753.

Chapman, RL. 1984. An assessment of the current state of our knowledge of the Trentepohliaceae. In: Systematics of the Green Algae (Irvine, D.E.G. Irvine, John, D.M., eds.). Academic Press, London, pp. 233-250.

Chapman, RL, Good BH. 1983a. Ultrastructure of plasmodesmata and cross walls in *Cephaleuros*, *Phycopeltis*, and *Trentepohlia* (Chroolepidaceae, Chlorophyta). Bristish Phycological Journal. 13: 241-246.

Chapman, RL, Good BH. 1983b. Subaerial symbiotic green algae:interactions with vascular plant hosts. In: Algal Symbiosis: A Continuum of Interaction Strategies (Goff, LJ., ed.). Cambridge University Press, NY, pp. 173-204.

Chapman RL, Waters DA. 2002. Lichenization of the Trentepohliales. In: Symbiosis (Seckbach, J., ed.). Kluwer Academic Publishers, The Netherlands, pp. 359–371

López-Bautista JM, Waters DA, Chapman RL. 2002. The Trentepohliales revisited. Constancea 83. http://ucjeps.berkeley.edu/constancea/83/ lopez_etal/trentepohliales. html.

Mollenhauer HH. 1964. Plastic embedding mixtures for use in electron microscopy. Stain Technology. 39:111-114.

Nelson SC. 2008. *Cephaleuros* species, the plant-parasitic green algae. Plant Disease. 43:1–6.

Ponmurugan P, Saravanan D, Ramya M. 2010. Culture and biochemical analysis of a tea algal pathogen *Cephaleuros parasiticus*. Journal of Phycology. 46: 1017–1023.

O'Kelly CJ, Floyd GL. 1990. Chlorophyte Orders of Uncertain Affinities, Order Prasiolales. In: Handbook of Protoctista (Margulis L, Corliss JO, Melkonian M, Chapman DJ, eds.). Jones and Bartlett Publishers, Boston, pp 658-660.

Ramya M, Ponmurugan P, Saravanan D. 2013. Management of *Cephaleuros parasiticus* Karst (Trentepohliales: Trentepohliaceae), an algal pathogen of tea plant, *Camellia sinsensis* (L.) (O. Kuntze). Crop Protection. 44:66–74.

Timpano P, Pearlmutter NL. 1983. Algal invasion of angiosperm mesophyll. Scanning Electron III. 1511-1517.

Silva PC. 1952. A review of nomenclatural conservation in the algae from the point of view of the type method. University of California Publications in Botany. 25:214-324.

Sluiman HJ. 1989. The green algal class Ulvophyceae: an ultrastructural survey and classification. Cryptogamie Algologie. 1:83-94.

Thompson RH, Wujek DE. 1997. Trentepohliales: *Cephaleuros*, *Phycopeltis*, and *Stomatochroon*, Morphology, Taxonomy and Ecology. Scientific Publishers, Inc., Lebanon, NH. 149 pp.

Zhu H, Zhao Z-H, Xia S, Hu Z-Y, Liu G-G. 2014. Morphology and phylogenetic position of Stomatochroon reniformis var. chinensis var. nov. (Trentepohliales, Ulvophyceae), a rare endobiotic alga from China. Phycologia. 53:493-501.

80TH ANNUAL MEETING

THAD COCHRAN CONVENTION CENTER
HATTIESBURG, MS

FEBRUARY 18-19TH, 2016

SUBMIT ABSTRACTS BY NOV. 1, 2015

Make sure to Renew Your Membership

Can also be done on-line at : http://msacad.org/

Membership/Registration opens December 1, 2015

Renew and join early to avoid late fees

MISSISSIPPI ACADEMY OF SCIENCES ABSTRACT FORM/MEMBERSHIP FORM

ABSTRACT INFORMATION

Abstract title:_____
Name of Presenting Author(s): _____
If you are a student please fill-out the next line
Name of Mentor and e-mail of Mentor _____
(Presenter must be current (i.e., 2016 membership dues must be paid), student member, regular member or life member of the MAS)
Telephone_____Email_____

Check the division in which you are presenting

__ Agriculture and Plant Science
__ Cellular, Molecular, and Dev. Biol
__ Chemistry and Chem. Engineering
__ Ecology and Evolutionary Biology
__ Geology and Geography
__ Health Sciences
__ History and Philosphy of Sciences
__ Math., Computer Sci and Statistics
__ Marine and Atmospheric Sciences
__ Physics and Engineering
__ Psychology and Social Sciences
__ Science Education
__ Zoology and Entomology

Complete either the Membership/Pre-Registration form if you plan to attend and present at the meeting if you do not plan to attend the meeting please complete the membership form

MEMBERSHIP/ PRE-REGISTRATION INFORMATION
New ___ Renewal___
Mr. Ms. Dr._____
Address _____
City, State, Zip _____
School or Firm _____
Telephone_____ **Email**_____

PLEASE INDICATE DIVISION YOU WISH TO BE AFFILIATED _____
Before January 15, 2016…….Regular Member/Pre-Registraion $130 Student Member/ Pre-registration $50
After January 15, 2016…….Regular Member/Registraion $170 Student Member/ Pre-registration $60

MEMBERSHIP INFORMATION
New ___ Renewal___
Mr. Ms. Dr._____
Address _____
City, State, Zip _____
School or Firm _____
Telephone_____ **Email**_____

PLEASE INDICATE DIVISION YOU WISH TO BE AFFILIATED _____
Regular Member $30 **Student Member $10** **Life Member $450**
Educational Member $550 **Corporate Patron $1000** **Corporate Donor $500**

CHECKLIST
Please complete the following:
__ Enclose title of abstract (even if abstract has been submitted electronically)
__ Complete membership/registration form (this form)
__ Enclose the following payments (Make checks payable to Mississippi Academy of Sciences)
__ $25 per abstract
__ $130 regular membership/pre-registration fee OR $50 student membership/pre-registration fee
__ You must supply a check #_____ or P.O. #_____ (or indicate Pay Pal confirmation) _____

MISSISSIPPI ACADEMY OF SCIENCES—ABSTRACT INSTRUCTIONS
PLEASE READ ALL INSTRUCTIONS BEFORE YOU SUBMIT YOUR ABSTRACT ON-LINE

- Your paper may be presented orally or as a poster. Oral presentations are generally 15 minutes. The speaker should limit the presentation to 10-12 minutes to allow time for discussion; longer presentations should be limited accordingly. Instructions for poster presentations are linked here.
- Enclose a personal check, money order, institutional check, or purchase order for $25 publication charge for each abstract to be published, payable to the Mississippi Academy of Sciences. The publication charge will be refunded if the abstract is not accepted.
- The presenting author must be a member of the Academy at the time the paper/poster is presented. Payment for membership of one author must be sent for the abstract to be accepted.
- Attendance and participation at all sessions requires payment of registration.
- Note that three separate fees are associated with submitting and presenting a paper at the annual meeting of the Mississippi Academy of Sciences.
    1. An abstract fee is assessed to defray the cost of publishing abstracts and
    2. A membership fee is assessed to defray the costs of running the Academy.
    3. Membership/Preregistration payment ($130 regular; $50 student) may accompany the abstract, or you may elect to pay this fee before January 15th, or pay full late membership/registration fees at the meeting ($170 regular, $60 student).
- Abstracts may **only** be submitted on line via a link through the MAS website.The appropriate abstract fees can be paid via Paypal or sent via mail to Barbara Holmes at the Academy address.
- **Late abstracts will be accepted with a $10 late fee during November increased to $25 after that. Late abstracts will be accepted only if there is room in the appropriate division. They will be published in the April issue of the MAS JOURNAL.**
- Submit your appropriate fees NO LATER THAN January 15th, 2016.

Ms. Gerri Wilson
Mississippi Academy of Sciences
Post Office Box 55907
Jackson, MS 39296-5907

GUIDELINES FOR POSTER PRESENTATIONS

- The Academy provides poster backboards. Each backboard is 34" high by 5' wide. Mount the poster on the board assigned to you by your Division Chairperson. Please do not draw, write, or use adhesive material on the boards. You must provide your own thumb tacks.
- Lettering for your poster title should be at least 1" high and follow the format for your abstract. Lettering for your poster text should be at least 3/8" high.
- Posters should be on display during the entire day during which their divisional poster session is scheduled. They must be removed at the end of that day.
- Authors must be present with their poster to discuss their work at the time indicated in the program.

Author Guidelines

Editorial Policy. The Editorial Board publishes articles on all aspects of science that are of general interest to the scientific community. General articles include short reviews of general interest, reports of recent advances in a particular area of science, current events of interest to researchers and science educators, etc. Research papers of sufficiently broad scope to be of interest to most Academy members are also considered. Articles of particular interest in Mississippi are especially encouraged.

Research papers are reports of original research. Submission of a manuscript implies that the paper has not been published and is currently at the time of submission being considered for publication elsewhere. At least one of the authors must be a member of the Academy, and all authors are encouraged to join.

Manuscripts. Submit the manuscript electronically to the Mississippi Academy of Sciences under your profile in the member location of the website. Please also provide a cover letter to the Editor of the Journal. The cover letter should authorize publication: give the full names, contact information, for all authors; and indicate to whom the proofs and correspondence should be sent. Please notify the Editor on any changes prior to publication.

Manuscripts must adhere to the following format:

- One inch margins on 8.5 x 11 inch paper;
- Text should be left-justified using twelve point type;
- Double spaced throughout, including the title and abstract;
- Arabic numerals should be used in preference to words when the number designates anything that can be counted or measured (7 samples, 43 species) with 2 exceptions:
- To begin a sentence (Twenty-one species were found in…)
- When 2 numeric expressions are adjacent in a sentence. The number easiest to express in words should be spelled out and the other left in numeric form (The sections were divided into eight 4-acre plots.).
- Measurements and physical symbols or units shall follow the International System of Units (SI *Le Système international d'unités*) with metric units stated first, optionally followed by United States units in parentheses. *E.g.*: xx grams (xx ounces); and
- Avoid personal pronouns.

Format

Abstract. In 250 or fewer words summarize any new methods or procedures critical to the results of the study and state the results and conclusions.

Introduction. Describe the knowledge and literature that gave rise to the question examined by, or the hypothesis posed for the research.

Materials and methods. This section should describe the research design, the methods and materials used in the research (subjects, their selection, equipment, laboratory or field procedures), and how the findings were analyzed.

Results. The text of the results should be a descriptive narrative of the main findings, of the reported study. This section should not list tabulated data in text form. Reference to tables and figures included in this section should be made parenthetically in the text.

Discussion. In this section compare and contrast the data collected in the study with that previously reported in the literature. Unless there are specific reasons to combine the two, as explained by the author in the letter of transmittal, Results and Discussion should be two separate sections.

Acknowledgments. Colleagues and/or sources of financial support to whom thanks are due for assistance rendered in completion of the research or preparation of the manuscript should be recognized in this section rather than in the body of the text.

Literature cited. List references alphabetically. Cite references in the text by author and year of publication (e.g., Smith, 1975; Black and Benghuzzi, 2011; Smith et al., 2010; Smith, 2011a, 2011b). The following examples illustrate the style to be used in the literature list.

Black DA, Lindley S, Tucci M, Lawyer T, Benghuzzi H. A new model for the repair of the Achilles tendon in the rat. J Invest Surg. 2011; 24(5): 217-221.

Pearson HA, Sahukhal GS, **Elasri** MO, Urban MW. Phage-bacterium war on polymeric surfaces: can surface-anchored bacteriophages eliminate microbial infections? Biomacromolecules. 2013 May 13;14(5):1257-61.

Bold, H.C., C.J. Alexopoulos, and T. Delevoryas. 1980. Morpholgy of plants and fungi, 4th ed. Harper and Row, New York. 819 pp

Web-page

- name of author(s) -if known
- title of the work - in quotes, if known
- title of the Web page - in italics, if applicable
- date of last revision
- URL
- Date accessed

Example:

Ackermann, Ernest. "Writing Your Own Web Pages." *Creating Web Pages.* 23 Oct. 1996. http://people.umw.edu/~ernie/writeweb/writeweb.html 10 Feb. 1997.

File available by anonymous FTP

- name of author(s) -if known
- title of the work - in quotes, if known
- date of last revision
- URL
- Date accessed

Example:
American Civil Liberties Union. "Briefing paper Number 5, Drug Testing in the Work Place." 19 Nov. 1992. ftp://ftp.eff.org/pub/Privacy/Medical/aclu_drug_testing_workplace.faq 13 Feb. 1997.

Please Tables and Figures at the end of the manuscript submitted.

Tables. Tables must be typed double spaced, one table to a page, numbered consecutively, and placed at the end of the manuscript. Since tables must be individually typeset, consolidation of data into the smallest number of tables is encouraged. A horizontal double underline should be made beneath the title of the table, and single underlines should be made the width of the table below the column headings and at the bottom of the table. Do not use vertical lines, and do not place horizontal lines in the interior of the table. Use footnotes, to clarify possible questions within the table, should be noted by asterisks, daggers, or other symbols to avoid confusion with numerical data. Tables should be referred to parenthetically in the text, for example (Table 1).

Figures and illustrations. Figures may be photographs, computer -generated drawings, or graphs and should be placed at the end of the manuscript and referenced in the appropriate place.. All illustrations are referred to as “Figures” and must be numbered consecutively. Illustrations other than those generated by the author(s) must include permission for use and credit to the originator. Each figure must have a complete legend that is typed, double-spaced, on a separate sheet which precedes the figures in the manuscript. Figures should be referred to parenthetically in the text, for example (Fig. 1).

Footnotes. Text footnotes **should not be used**

Submission Preparation Checklist

As part of the submission process, authors are required to check off their submission's compliance with all of the following items, and submissions may be returned to authors that do not adhere to these guidelines.

1. The submission has not been previously published, nor is it before another journal for consideration (or an explanation has been provided in Comments to the Editor).
2. The text adheres to the stylistic and bibliographic requirements outlined in the Author Guidelines.
3. I acknowledge that if my manuscript is peer-reviewed and accepted for publication, there will be a paper charge fee of $50/page for **non-Academy members**.
4. The manuscript file is in Microsoft Word format.

Copyright Notice

Authors who publish with this journal agree to the following terms:

1. Authors retain copyright and grant the journal right of first publication
2. Authors are able to enter into separate, additional contractual arrangements for the non-exclusive distribution of the journal's published version of the work (e.g., post it to an institutional repository or publish it in a book), with an acknowledgement of its initial publication in this journal.
3. Authors are permitted and encouraged to post their work online (e.g., in institutional repositories or on their website) prior to and during the submission process, as it can lead to productive exchanges, as well as earlier and greater citation of published